

Michigan Institute for Plasma Science and Engineering (MIPSE)

16th ANNUAL GRADUATE STUDENT SYMPOSIUM

December 3, 2025 University of Michigan North Campus, Ann Arbor, MI 48109

Schedule

I. Special MIPSE Seminar

Johnson Rooms, 3213 Lurie Engineering Center, 1221 Beal Avenue

1:00 – 1:25 pm	Registration, light lunch
1:25 – 1:30 pm	Prof. Mark J. Kushner , University of Michigan Director, MIPSE <i>Opening remarks</i>
1:30 – 2:30 pm	Prof. David Ruzic, University of Illinois, Urbana-Champaign Winner, University of Michigan Plasma Prize 2024 What do Fusion Technology, Physical Vapor Deposition and EUV Lithography Have in Common?

II. Poster Presentations

Atrium, **EECS Building**, 1301 Beal Avenue

5:45 – 6:00 pm	Best Presentation Award ceremony
5:30 – 5:45 pm	Poster removal
4:45 – 5:30 pm	Poster Session III
4:00 – 4:45 pm	Poster Session II
3:15 – 4:00 pm	Poster Session I
2:45 – 3:15 pm	Poster setup

Participating institutions:

University of Michigan, Michigan State University, University of Notre Dame.

Poster Session I

1-01	Madison Allen	U-M	Optimal Diagnostic Placement for Calibrating a Hall Thruster Model on Orbit
1-02	Cole Stewart	MSU	The Effect of Macroparticle Weight Factor on Particle-in-
			Cell Simulations in Low Temperature Plasmas
1-03	Bineet Dash	U-M	Plasma Field Diagnostics using Rydberg
			Electromagnetically Induced Transparency
1-04	Chelsea Tischler	U-M	Generation of Diffuse Reactive Oxygen Plasma in an
			Atmospheric Pressure Plasma Jet
1-05	Evan Litch	U-M	Dissociation and Ionization of Molecular Hall Thruster
			Propellants
1-06	Lan Jin	U-M	Photon-Assisted Thermionic Emission: A Theoretical
			Prediction for Photoelectron Energy Spectra, Emission
			Current, and Quantum Efficiency
1-07	Ari Eckhaus	U-M	Direct Measurements of Near-Field Electron Temperatures
			in an ECR Thruster
1-08	Horacio Moreno	U-M	Computation of Potential Magnetic Fields in the Solar
	Montanes		Corona with Integral Equation Methods
1-09	Ryan Park	U-M	Numerical Thermalization in 3D Particle-in-cell Simulations
1-10	Andrew Schok	U-M	Carbon Backsputter Mitigation with a Cusped Field
			Retarding Beam Dump
1-11	Alexander Loomis	MSU	Chemical Vapor Deposition of Silicon Vacancy Ensembles in
			Low Strain Diamond with a NIRIM Type Reactor
1-12	Amelia Lee	U-M	Impact of Ionospheric Mesoscale Flow Enhancements on
			Polar Cap Patch Propagation
1-13	James Welch	U-M	Molecular Dynamics Simulations of Temperature
			Relaxation in Strongly Magnetized, Antiproton-Electron
			Plasmas
1-14	Md Mashrafi	U-M	Two-Frequency RF Fields Induced Multipactor in Coaxial
			Transmission Line
1-15	Alexander Cushen	U-M	Do Mercury's Dipolarization Fronts Originate from Flux
			Ropes? MHD-AEPIC Simulations of Mercury's
	-		Magnetosphere
1-16	Kyle Kemmerer	U-M	Molecular Dynamics Simulations of Electrical Conductivity
			in Strongly Magnetized Plasmas
1-17	Ibukunoluwa	ND	Homogeneous vs. Plasma Chemistry in High Temperature
	Akintola		Methane DBDs: A Global Kinetic and Graph Theory Analysis

Poster Session II

2.04	\A/:II: B.#	11.54	Interference and a minute of the state of the Developer
2-01	William Maxon	U-M	Interface-preserving Numerical Methods for Radiation Hydrodynamics
2-02	Wencheng Lin	MSU	Zero-Dimensional Plasma–Catalysis Model for Surface
			Coverage of Nitrogen and Oxygen Atoms
2-03	Nicolas Kalem	U-M	Harnessing Ionization Effects for Direct Laser Acceleration
			of Electrons
2-04	Yeon Geun Yook	U-M	Effect of a Rectangular Bias Waveform on Cryogenic
			Plasma Etching of SiO ₂
2-05	Md Arifuzzaman	U-M	Anisotropic Charge Transport and Current Crowding in
	Faisal		Vertical Thin-Film Contacts with 2D Layered Materials
2-06	Briggs Damman	U-M	Molecular Dynamics Simulation of Hydrodynamic
			Transport Coefficients in Plasmas
2-07	Declan Brick	U-M	Model Based Investigation of Self-Consistent Closure in a
			Hall Thruster Model
2-08	Mitchell Indek	U-M	Effects of Europa's Atmosphere on Its Magnetic and
			Plasma Environment: Application of Multi-Fluid MHD
			Simulations to Spacecraft Flybys
2-09	Nolan Tribu	U-M	Space Plasma Dynamics and the Resulting Energy Flux into
			Earth's Magnetosphere
2-10	Miron Liu	U-M	Experimental Demonstration of a Spatial Anti-aliasing
			Plasma Wave Analysis Technique on Ion Acoustic
			Turbulence in a Hollow Cathode Plume
2-11	Khalil Bryant	U-M	Complexity Analysis of a CT Injection Experiment on BRB
2-12	Yifan Gui	U-M	Pulsed Power Strategies for Plasma Etching of High Aspect
			Ratio Features Using Fluorocarbon Gas Mixture for
			Feature Charging Control
2-13	Md Wahidur	MSU	Effects of Annular Beam Properties on Gap Coupling in
	Rahman		High-Frequency Microwave Devices
2-14	Jarett LeVan	U-M	Foundations of Magnetohydrodynamics with Applications
			to Dense Plasmas
2-15	Mary Smirnova	U-M	Fusing Ground-Based and GOLD Inferred TEC Using
	_		Statistical Calibration
2-16	Oluwatosin Ohiro	U-M	Multiscale Modeling of Radical and Vibrational Pathways
			in Plasma-Assisted Ammonia Synthesis on Fe (110) and Ni
			(111)
2-17	Chenyao Huang	U-M	Charging Dynamics During Pulsed Plasma Etching of High
			Aspect Ratio Features in Dielectric Materials
1	1	1	1 •

Poster Session III

3-01	Alexandra Roosnovo	U-M	Heavy-Ion Plasma Properties During Rotationally-Driven Interchange Events: Insights from Juno Observations at Jupiter
3-02	Kwyntero Kelso	U-M	X-ray Absorption Spectroscopy Measurements of Radiatively Ionized Argon Gas
3-03	Michelle Bui	U-M	Observations & Modeling of Subauroral Sporadic-E Plasma Irregularities
3-04	Sankhadeep Basu	MSU	Femtosecond TALIF Measurements of Atomic Hydrogen in a Dielectric Barrier Discharge for Biodiesel Hydrogenation
3-05	John Riley O'Toole	U-M	Efficiency Mode Characterization of an Electron Cyclotron Resonance Magnetic Nozzle Thruster Operating on Nitrogen
3-06	Sarah Feldman	U-M	Boundary Layer Phenomena in Mercury's Magnetosphere
3-07	Jisu Jeon	U-M	PFAS Degradation in Water using Atmosphere Pressure Plasmas
3-08	Lucas Babati	U-M	Kinetic Theory of Warm Dense Matter
3-09	Grace Zoppi	U-M	Experimental Characterization of the Co-Axial Electrodeless Magnetoplasmadynamic Thruster
3-10	lan Freeman	MSU	Effects of Resistivity and Radiative Losses on Magnetic Reconnection in MHD
3-11	Julian Kinney	U-M	Spectral Line Widths in Plasmas using an Average Atom Model
3-12	Gonçalo Amadeu Mendes Cardoso	U-M	Controlling Energetic Neutral Beams Produced from Inductively Coupled Plasmas for Material Processing Applications
3-13	Yves Heri	U-M	Space-Charge and Circuit-Induced Distortion of Short-Pulse Beams in a Vacuum Diode
3-14	Joshua Latham	U-M	Control of Magnetic Reconnection in Laser Plasma Interaction
3-15	Jiashu Han	U-M	Vlasov-Poisson Simulations of Ion Acoustic Waves
3-16	Bingqing Wang	U-M	Curvature-Enhanced Quantum Tunneling Emission in Dissimilar Metal-Insulator-Metal Junctions

Abstracts: Poster Session I

Optimal Diagnostic Placement for Calibrating a Hall Thruster Model on Orbit* Madison Allen and Benjamin Jorns

University of Michigan, Aerospace Engineering (mgallen@umich.edu)

Experimental design is a key consideration for the validation and calibration of engineering models of Hall effect thrusters. Hall Effect thrusters are in-space propulsion devices predominantly employed for station keeping and deep space missions. They are also one of the proposed technologies for future crewed missions to Mars due to their high thrust density and acceptable efficiency. One limiting factor for Hall thruster application is the well-observed difference in performance between ground tests and space flight. These devices typically operate in vacuum

testing facilities to allow for plasma generation and to imitate on-orbit performance. However, these ground testing facilities do not replicate space background pressures due to their limited pumping speeds. Multiple studies exist as attempts to characterize the changes in performance as a consequence of high background pressures by increasing the background pressure to various quantities then performing diagnostics and extrapolating the results to space conditions [1-3]. This process is limited by the amount of data required for confident extrapolation and the ability to reach a large range of pressure conditions. Another approach is to fasten diagnostics to the spacecraft and measure thruster behavior in orbit [4]. The number of diagnostics as well as the number of measurement positions are extremely limited during flight. Therefore. these measurements are unable to calibrate Hall thruster models. Thus, there is an apparent need to determine a set of specific diagnostics and their placement location that are able to calibrate a Hall thruster model with minimal uncertainty.

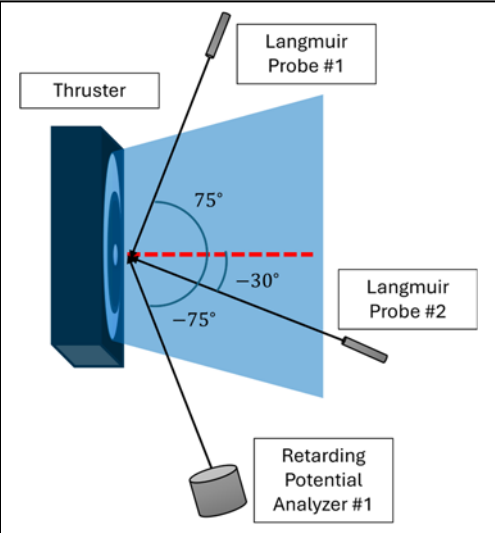


Figure 1 - An example of a set of probe diagnostics placed in optimal positions with respect to the thruster selected using OED.

In this work, we apply the Optimal Experimental Design (OED) algorithm to determine the type of data necessary for model regression. [5] Certain measurement locations and data types can improve the calibration more than others, and this algorithm will determine the best configuration. We select experiments for calibrating a predictive engineering model for Hall thrusters (PEM) developed by Eckels et al. [6]. It incorporates a 1D Hall Thruster code that models the near-field dynamics and thruster performance, a model for the cathode coupling voltage, and a model for the far-field ion current density. The model depends on variables such as the background pressure, flow rates, and thruster dimensions. To determine the optimal experiments we calculate the Expected Information Gain of various sets of diagnostics and their respective positions using the model [5]. With this work we are able to identify a package for diagnostics during flight operation for the SPT-100 Hall thruster that will acquire the most informative data for model regression.

* Work supported by the NASA Space Technology Graduate Research Opportunity.

- [1] Diamant, K. D., Liang, R., and Corey, R. L., "The Effect of Background Pressure on SPT-100 Hall Thruster Performance," 50th AIAA/ASME/SAE/ASEE Joint Propulsion Conference, American Institute of Aeronautics and Astronautics, 2014.
- [2] Huang, W., Kamhawi, H., and Haag, T., "Effect of Background Pressure on the Performance and Plume of the HiVHAc Hall Thruster," 33rd International Electric Propulsion Conference, 2013.
- [3] Byers, D., and Dankanich, J., "A Review of Facility Effects on Hall Effect Thrusters," 31st International Electric Propulsion Conference, 2009.
- [4] Manzella, D., Jankovsky, R., Elliot, F., Mikellides, I., Jongeward, G., and Allen, D., "Hall Thruster Plume Measurements On-Board the Russian Express Satellites," 27th International Electric Propulsion Conference, 2001.
- [5] Huan, X., and Marzouk, Y. M., "Simulation-based optimal Bayesian experimental design for nonlinear systems," Journal of Computational Physics, Vol. 232, 2013, pp. 288–317.
- [6] Eckels, J., Marks, T., Allen, M., Jorns, B., and Gorodetsky, A., "Hall thruster model improvement by multidisciplinary uncertainty quantification," Journal of Electric Propulsion, Vol. 3, 2024, p. 19.

The Effect of Macroparticle Weight Factor on Particle-in-Cell Simulations in Low Temperature Plasmas*

Cole Stewart ^a and John Verboncoeur ^b

- (a) Department of Computational Mathematics Science and Engineering and Department of Physics and Astronomy, Michigan State University, East Lansing, MI 48823 USA (stewa873@msu.edu)
- (b) Department of Computational Mathematics Science and Engineering and Department of Electrical and Computer Engineering, Michigan State University, East Lansing, MI 48823 USA (johnv@msu.edu)

Fully kinetic Particle-in-Cell/Monte Carlo Collisions (PIC/MCC) is an essential tool in understanding the complex physics of plasmas (CPP). Numerical accuracy and stability are important for PIC/MCC simulations and have been the subject of studies since its conception. Recent work reported that the plasma density of explicit electrostatic PIC/MCC simulations at steady state diverges with decreasing macroparticle weight for low pressure CCPs [1]. The simulations in [2] suggest around a thousand macroparticles per cell is required for convergence, indicating a high computational cost, especially in 2D or 3D cases. In this work, we revisited the macroparticle weight issue and explored the dependence of the plasma discharge properties on the particle weight. We will explore the numerical effects and physics regime related to this issue and show the effect of implementing intracell Coulomb collisions.

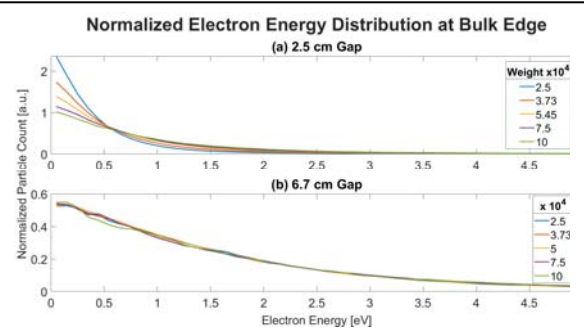


Figure 1 – Reverse Cumulative Electron Energy Distribution at the edge of the bulk for a few select cases of varying superparticle weight across the 2.5 cm and 6.7 cm gaps, respectively. The background argon pressure was 76 mTorr at 0.026 eV. The plasma was driven at 250V at 13.56 MHz, and the electrode was 1 cm². The cell count was 500 for each case, with Δx corresponding to the gap length divided by cell count.

*Work supported by AFOSR MURI Grant NO. FA 9550-21-1-0367 and NSF-DOE Partnership Grant for DE-SC0022078.

- [1] Vass, M, Palla, P, Hartmann, P 2022, Plasma Sources Science and Technology 31, no. 6, p. 064001.
- [2] E. Erden and I. Rafatov, Contributions to Plasma Physics 54, no. 7, pp. 626–634, Dec. 2013.

Plasma Field Diagnostics Using Rydberg Electromagnetically Induced Transparency*

<u>Bineet Dash</u>, Xinyan Xiang, Dingkun Feng and Georg Raithel Department of Physics, University of Michigan, Ann Arbor (bkdash@umich.edu)

We present a novel, non-invasive plasma field diagnostic technique based on Rydberg Electromagnetically Induced Transparency (EIT). Due to their large dipole moments, Rydberg atoms undergo Stark shifts in electric fields that are orders of magnitude greater than those in low-lying states. EIT is a coherent quantum interference effect that arises in multi-photon excitation to Rydberg levels via an intermediate state, wherein the Rydberg manifold is mapped to narrow transparency windows in the transmitted intensity of one of the driving lasers. Rydberg-EIT thus enables alloptical readout of Stark shifts, providing an atom-based, electrode-free method for electric field measurement with sub-V/cm sensitivity.

In this study, we demonstrate the use of Rydberg-EIT for *in-situ* electric field measurement in a continuous, low-pressure, inductively coupled Argon plasma, seeded with a trace of Rubidium (Rb) vapor as the local electric field sensor. By optically interrogating the embedded Rb atoms with narrow-linewidth diode lasers, we obtain Rydberg-EIT spectra within the plasma volume that exhibits strong screening of the applied RF field. From the measured spectra, we extract the Holtsmark microfield distribution and plasma electron density. Additionally, we measure the electromagnetic field generated by the inductor antenna inside the ICP chamber in the absence of a plasma discharge. Finally, we report on progress toward spatiotemporally resolved field mapping, with potential implications for diagnostics in dusty plasma.

^{*} This project was supported by the U.S. Department of Energy, Office of Science, Office of Fusion Energy Sciences under Award Number DE SC0023090.

Generation of Diffuse Reactive Oxygen Plasma in an Atmospheric Pressure Plasma Jet *

Chelsea M. Tischler and John E. Foster

University of Michigan (chemay@umich.edu)



Figure 1: Typical argon plasma jet with filament discharge.

Low temperature plasmas have many practical applications across a wide range of industrial, medical, and environmental sectors. One considerable challenge associated with the operation of these jets using reactive feed gas is the formation of hot filaments, which lead to nonuniformity in the efflux and can damage the substrate. Suppressing filaments is key to widespread implementation of plasma jets and could thereby eliminate the need for some low-pressure processes that require vacuum chambers and pumps. Presented here is a study of a nanosecond pulsed-DC plasma jet that operates at atmospheric

pressure using a mixture of argon and oxygen and produces a diffuse and reactive atomic oxygen plasma at the jet exit. This mode of operation holds potential for applications that have traditionally necessitated vacuum

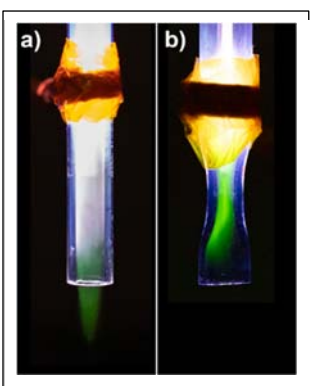


Figure 2: Diffuse and reactive atomic oxygen plasma produced in a ns pulsed dc jet with argon as the primary gas with a) cylindrical tube geometry, and b) a cylindrical tube with a CD nozzle geometry.

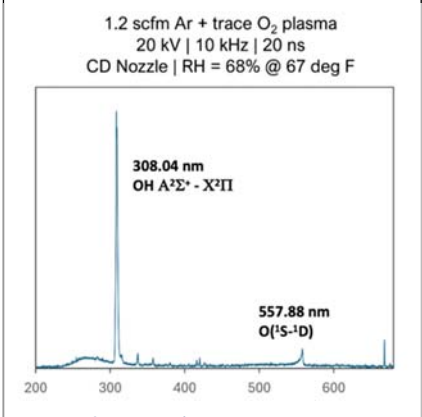


Figure 3: Optical emission spectroscopy demonstrates presence of highly reactive OH and atomic O.

absence of filaments within jet plume. Emission spectroscopy is performed to analyze the effluent while starch iodine tests reveal the reactive nature of the jet, marking a significant milestone in the preliminary development of this device.

conditions. In this work, we employ traditional and high-speed imaging techniques to characterize the parameter space (voltage, frequency, pulse width, gas flow, gas blend) and to demonstrate the

^{*} Work supported by the NSF ECLIPSE program.

Dissociation and Ionization of Molecular Hall Thruster Propellants*

Evan Litch a, Greg Armstrong b, Anna Nelson b, Elaine Petro c and Mark J. Kushner a

(a) University of Michigan, Ann Arbor, MI 48109-2122, USA(b) Quantemol, London EC1V 21NZ, United Kingdom(c) Cornell University, Ithaca, NY 14850, USA

Plasma propulsion devices such as hall thrusters (HTs) typically use Xe as the propellant due to its high mass and low ionization potential. However, due to the scarcity and cost of Xe, alternate fuels are being investigated which are also environmentally friendly and which are not potentially damaging to the spacecraft. Solutions containing, for example, TPA (tripropylamine, (CH₃CH₂CH₂)₃N) are attractive alternate fuels due to their ease of storage and low cost. However these complex molecules also result in complex plasma chemistry, producing a variety of ions that, when accelerated, produce thrust defined by the current and mass flow rate. For example, thermally decomposed, TPA-like mixtures with air may produce H₂O, NO_x, CO_x, and CH_x. These decomposition products are further dissociated when exposed to the plasma environment. To provide insights into the variety of ions produced using alternate fuels for plasma propulsions systems, simulations were conducted with the Hybrid Plasma Equipment Model (HPEM) in an HT-like geometry. A feedstock mixture containing H₂O/N₂/CH_x/CO₂, representative of TPA-like decomposition product propellants were investigated. The resulting dissociation products, ion densities, fluxes, and velocities will be discussed.

^{*} Work was supported by the United States Air Force Research Labs (FA9453-24-2-0007).

Photon-Assisted Thermionic Emission: A Theoretical Prediction for Photoelectron Energy Spectra, Emission Current, and Quantum Efficiency*

Lan Jin and Peng Zhang

Department of Nuclear Engineering and Radiological Science, University of Michigan, Ann Arbor, Michigan 48109, USA (umpeng@umich.edu)

Electron emission is important to many applications ranging from accelerators and ultrafast electron diffraction/microscopy to high-power microwave sources and electric propulsion. Photon-assisted thermionic emission (PATE) leverages optical excitation to amplify electron release from heated cathodes, enabling higher current density at a given temperature—or equivalent performance at lower heater power—than dark thermionics alone. In RF/DC electron guns [1], microwave tubes, and propulsion cathodes, optical assistance can reduce warm-up time and heater

load, relax vacuum requirements at a fixed current density, and help preserve cathode lifetime by lowering operating temperature. Key performance metrics include quantum efficiency (QE), energy spread, and cathode lifetime, which together define application-specific trade-offs [2-3].

In this work, we investigate PATE from tungsten (W) and lanthanum hexaboride (LaB₆)—refractory emitters with different work functions—using a quantum model that solves the one-dimensional Schrödinger equation exactly [4-5]. We explore the photoelectron energy spectra, emission current and QE in varying temperature, laser wavelength and optical field amplitude. As shown in Fig. 1, we present photoelectron spectra for W at 800 nm with peak optical fields $F_1 = 0, 0.01, 0.1, 0.5 \text{ V/nm}$ across varying temperatures, highlighting the transition from purely thermionic to photon-assisted and strong photon driven regimes.

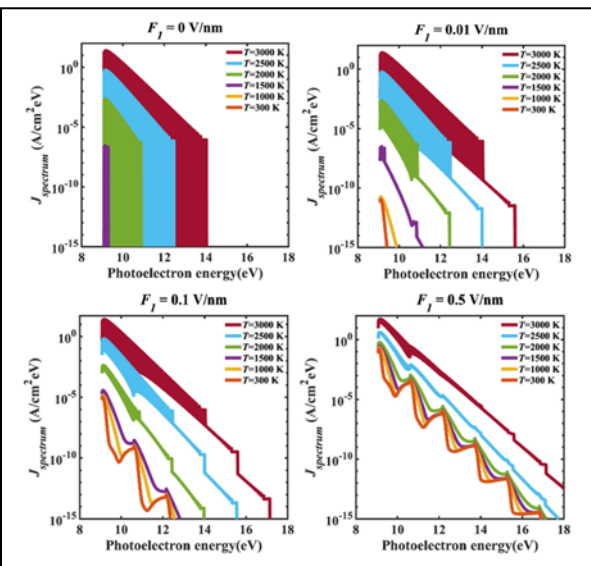


Figure 1 – Photoelectron energy spectra at various temperature for peak laser strength F_1 of 0, 0.01, 0.1, and 0.5 V/nm at wavelength 800 nm.

* Work supported by the Air Force Office of Scientific Research (AFOSR) Grant No. FA9550-20-1-0409, the Air Force Office of Scientific Research (AFOSR) Grant No. FA 9550-22-1-0523, and National Science Foundation (NSF) Grant No. 2516752.

- [1] Jin, Lan, Yang Zhou, and Peng Zhang, Journal of Applied Physics 134.7 (2023).
- [2] Torgasin, K., et al., Physical Review Accelerators and Beams 20, 073401 (2017)
- [3] Riffe, D. Mark, et al., Journal of the Optical Society of America B 10, 1424-1435 (1993)
- [4] P. Zhang, and Y.Y. Lau, Sci. Rep. **6**(1), 19894 (2016).
- [5] Zhou, Yang, and Peng Zhang, Journal of Applied Physics 130.6 (2021).

Direct Measurements of Near-Field Electron Temperatures in an ECR Thruster

Ari Eckhaus and Benjamin Jorns

University of Michigan (aeckhaus@umich.edu)

Electron cyclotron resonance (ECR) thrusters are one of the most promising technologies for small-satellite electric propulsion. These devices operate by coupling microwave power into the electrons of a plasma. The thermal energy of the electrons is then converted into directed ion kinetic energy using a diverging magnetic field, referred to as a magnetic nozzle. Because of this principle of operation, determining the temperature of the electrons is critical to understanding both the microwave power coupling scheme and the magnetic nozzle's acceleration scheme.

Despite its importance, electron temperature in the plasma source region, where the electron cyclotron resonance interaction takes place, has yet to be measured experimentally. The difficulty with this measurement arises from the combination of high electron temperatures (~70 eV) and relatively small length scales (~10 mm). These two factors make conventional diagnostics, such as Langmuir probing, difficult to perform accurately, and highly perturbative to thruster operation.[1] Therefore, in this work we leverage non-invasive laser diagnostics to directly measure both the electron and ion properties near the plasma source region of an ECR thruster.

'The experimental setup used in this work is shown in Figure 1. The two laser diagnostics we utilize are Laser Induced Florescence (LIF) and Incoherent Thomson Scattering (ITS). Using LIF, we can measure the ion velocity distribution function (IVDF). On the other hand, ITS allows us to determine the electron energy distribution function (EEDF) and the corresponding electron temperature.[2] From these measurements, we will quantify efficiencies of the ECR stage and magnetic nozzle.

We will perform these experiments on the UM ECR V. II thruster. This test article nominally operates on xenon propellant at powers ranging

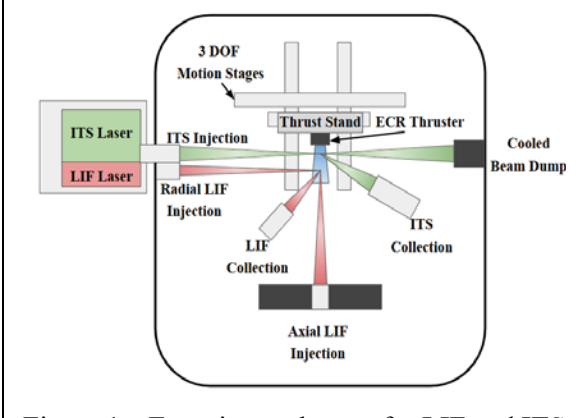


Figure 1 – Experimental setup for LIF and ITS laser diagnostics.

from 20 W to 50 W. We will measure the IVDF and EEDF as a function of axial position to investigate the conversion of electron thermal energy into ion kinetic energy in the magnetic nozzle. Additionally, by repeating these measurements under various thruster operating conditions, we will quantify the relationship between electron temperature and thruster delivered power and propellant flow rate.

Despite their theoretical promise, poor overall efficiency has largely limited the application of ECR thrusters. The laser diagnostics used in this work provide novel measurements of the electron and ion properties in the near-field plume region of the ECR thruster. This lends valuable insight to the power coupling and energy conversion processes, enabling us to better understand and quantify the loss mechanisms in these devices.

* Work supported by AFOSR Grant FA9550-25-1-0025.

- [1] S. Correyero et. al, PSST. 28, 9 (2019).
- [2] P. Roberts, Ph.D Thesis, Univ. of Mich. (2024).

Computation of Potential Magnetic Fields in the Solar Corona with Integral Equation Methods

Horacio Moreno Montañes and Robert Krasny

University of Michigan (hmorenom@umich.edu)

Understanding the mechanisms by which solar wind is heated in the solar corona is an important aspect of space weather forecasting and the prediction of solar magnetic events [1]. Current methods that solve the MHD equations modeling the solar corona [2] require the computation of the potential magnetic field to be used as an initial condition and to enforce boundary conditions. Currently, the magnetic field is computed from synchronic magnetogram data using either spherical harmonics or finite difference methods [3]. Finite difference solvers address the most important drawbacks from spherical harmonics approaches: the ringing in concentrated magnetic field regions and resolution close to the poles. However, computation is still limited by system size which can be large for the 3D grid used, and computation time can be long even when parallelized with several CPUs.

The potential can be formulated in terms of an integral equation involving the boundary conditions and a suitable Green's function [4]. Computing the potential is then done by discretizing the resulting integral as a direct sum. The runtime of this computation can be improved significantly by parallelization and the use of a GPU. Additionally, the use of a Barycentric Lagrange treecode [5] can reduce the operation count from $O(N^2)$ to $O(N \log N)$, allowing for better runtime for more refined grids. The purpose of this project is to develop and implement such a method to compute the solar potential magnetic field, and to compare with previous results [3] using alternate methods.

- [1] X. Liu, W. Liu, W.B.M. IV, D.T. Welling, G. Tóth, T.I. Gombosi, M.L. DeRosa, L. Bertello, A.A. Pevtsov, A.A. Pevtsov, K. Reardon, K. Wilbanks, A. Rewoldt, L. Zhao, Forecasting the 8 April 2024 Total Solar Eclipse with Multiple Solar Photospheric Magnetograms, (2025). https://doi.org/10.48550/arXiv.2503.10974.
- [2] B. Van Der Holst, I.V. Sokolov, X. Meng, M. Jin, W.B. Manchester, Iv, G. Tóth, T.I. Gombosi, ALFVÉN WAVE SOLAR MODEL (AWSoM): CORONAL HEATING, Astrophys. J. 782 (2014) 81. https://doi.org/10.1088/0004-637X/782/2/81.
- [3] G. Tóth, B. van der Holst, Z. Huang, Obtaining Potential Field Solutions with Spherical Harmonics and Finite Differences, (2011). https://doi.org/10.1088/0004-637X-732-2-102.
- [4] O.D. Kellogg, Electric Images; Green's Function, in: O.D. Kellogg (Ed.), Found. Potential Theory, Springer, Berlin, Heidelberg, 1967: pp. 228–248. https://doi.org/10.1007/978-3-642-86748-4 9.
- [5] N. Vaughn, L. Wilson, R. Krasny, A GPU-Accelerated Barycentric Lagrange Treecode, in: 2020 IEEE Int. Parallel Distrib. Process. Symp. Workshop IPDPSW, 2020: pp. 701–710. https://doi.org/10.1109/IPDPSW50202.2020.00125.

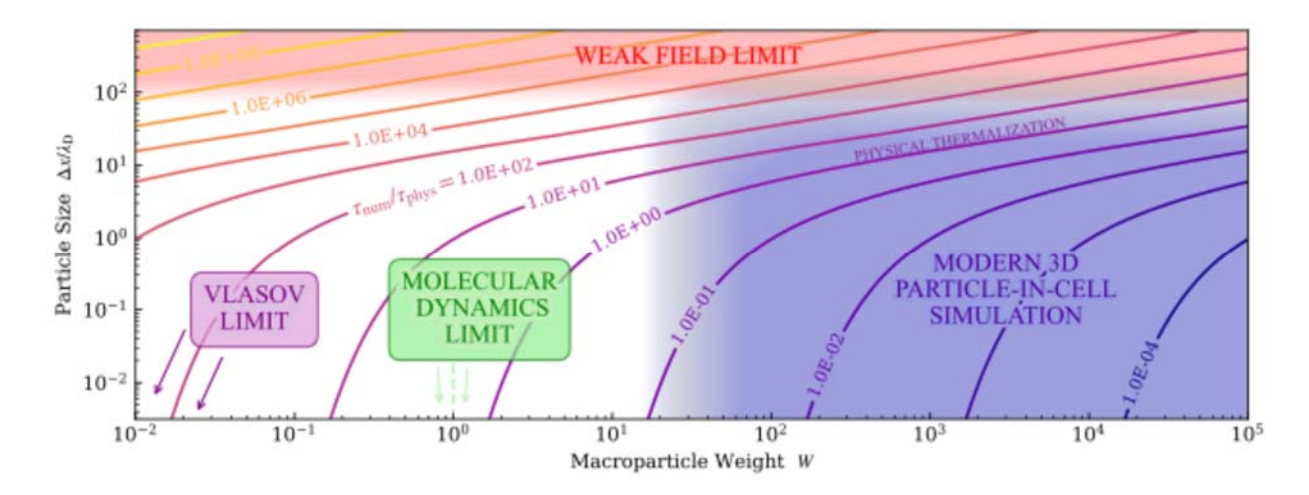
Numerical Thermalization in 3D PIC Simulations*

Ryan M. Park a, Chris Moore b, Scott D. Baalrud a

(a) Department of Nuclear Engineering and Radiological Sciences, University of Michigan, Ann Arbor, MI 48109, USA

(b) Sandia National Laboratories, Albuquerque, NM 87185, USA (rmpark@umich.edu)

A critical aim of particle-in-cell (PIC) simulations is to properly model the evolution of the velocity distribution function (VDF). Simulations with higher macroparticle weights have higher collision rates and corresponding rapid thermalization of the VDF. PIC methods are generally understood to compensate for this effect and provide a numerical solution to the collisionless Vlasov equation due to the weakened short-range force. This work tests the degree to which PIC effects compensate for large particle weights in 1-D, 2-D, and 3-D. It is determined that reaching the physical collision rate, let alone the Vlasov solution, in 3D PIC simulations may often be intractable for grids that resolve the Debye length. The collision time is calculated from PIC data and compared directly with the kinetic theory of Okuda, Birdsall, and Langdon in each of the three dimensions. This effect is distinct from grid heating and "particle noise" in the sense that energy conserving, δf, and quiet start methods do not inherently avoid numerical thermalization.



^{*} Sandia National Laboratories is a multimission laboratory managed and operated by National Technology & Engineering Solutions of Sandia, LLC, a wholly owned subsidiary of Honeywell International Inc., for the U.S. Department of Energy's National Nuclear Security Administration under contract DE-NA0003525.

Carbon Backsputter Mitigation with a Cusped Field Retarding Beam Dump*

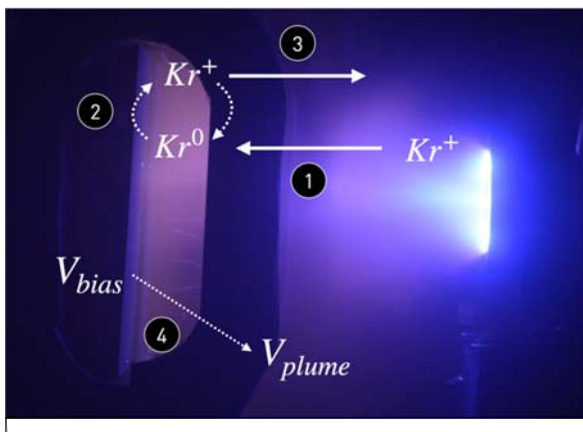
Braden Oh, <u>Andrew Schok</u>, Christopher McCullough, William Hurley, Collin Whittaker, Tate Gill, Thomas Marks and Benjamin Jorns

University of Michigan, Plasmadynamics and Electric Propulsion Laboratory, Ann Arbor, MI, 48105

The ability to electrostatically decelerate thruster beam ions as a means of reducing carbon backsputter in an electric propulsion test facility is experimentally evaluated. Previous work has

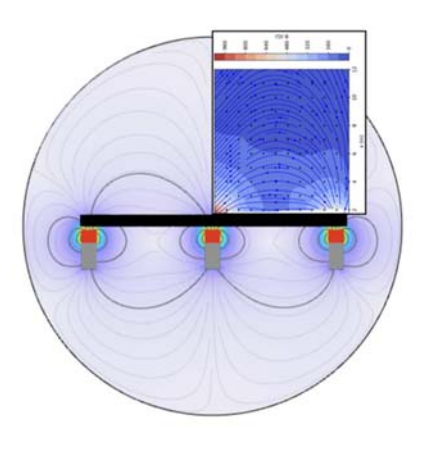
shown that while this type of ion-decelerating 'beam catcher' may reduce backsputter, it can confound deposition measurements by launching high-energy ions back at the thruster [1-2]. This study evaluates the effectiveness of canting the beam catcher in an effort to redirect backstreaming ions away from the thruster. The efficacy of this technique is evaluated by measuring the reduction in backsputter deposition/ion-induced erosion in the plane of the thruster with an electrostatically filtered quartz crystal microbalance (QCM). It is found that canting the beam catcher reduces the magnitude of backstreaming ion erosion by 64% when canting the beam catcher up to 27° with

respect to thruster centerline at a fixed bias of 150V and by 77% when canting the beam catcher up to 33° at a fixed bias of 125V [3]. While negative backsputter rates were not completely eliminated, it is shown through QCM data and a test employing grounded witness plates that this persistent erosion may be explained by the presence of low-energy background ions eroding material from grounded Key challenges and surfaces. limitation in the experimental configuration, particularly the use of a "guarded QCM" are discussed. The implications of these findings



Notional illustration by which new ions born via CEX are launched back at the thruster [1, 3].





Photograph of the cusped-field test article used in this study (left) and magnetic field simulation and measurement (right) [3].

and future avenues for probing and scaling beam catcher concepts are examined in the context of establishing ground-based high fidelity test environments.

* Work supported by the DARPA Talos Program, the NASA JANUS Institute, and the NSF GRFP.

- [1] Oh, et al. Carbon backsputter mitigation with a retarding beam dump. 38th IEPC Conf. (2024).
- [2] Thompson, et al. Methods for mitigating backsputter in electric propulsion test facilities i: Beam halter concept and design. AIAA SciTech Conf. (2024).
- [3] Oh, et al. Carbon backsputter mitigation with a cusped field retarding beam dump. 39th IEPC Conf. (2025).

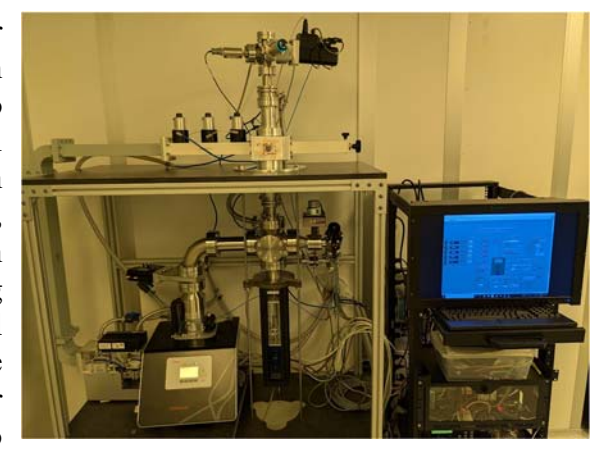
Chemical Vapor Deposition of Silicon Vacancy Ensembles in Low Strain Diamond with a NIRIM Type Reactor

<u>Alex Loomis</u> ^a, Logan Crooks ^a, Andrew R. Kirkpatrick ^a, Jonas N. Becker ^a and Shannon S. Nicley ^{a,b}

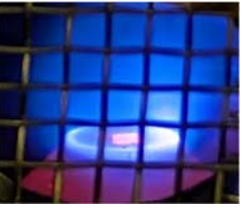
(a) Quantum Optical Devices Laboratory (QuOD), Michigan State University
(b) Fraunhofer USA Inc., Center Midwest, Coatings and Diamond Technologies Division,
1449 Engineering Research Ct. East Lansing, MI 48824, USA

In recent decades, improved technology and information theory have brought us closer to a second quantum revolution that utilizes quantum mechanics to its full potential [1]. Diamond is a great platform for optically active defects for quantum information processing (QIP) applications, able to host hundreds of different color centers within its wide bandgap. It is transparent from infrared to ultraviolet wavelengths and growth with ¹²C-enriched methane allows for nuclear spin-free material, suppressing spin-spin interactions to improve coherence times. The silicon vacancy (SiV) color center in diamond has particularly favorable properties for broadband quantum memories based on off-resonant Raman transitions. The SiV features inversion symmetry and large ground state splitting (50GHz) making it immune to first-order Stark shifts and large memory bandwidths [2]. The storage time of a quantum memory in a dense SiV ensemble is determined by its inhomogeneous broadening, and therefore the growth of high-quality material is needed.

Diamond growth through chemical vapor deposition (CVD) enables the fabrication of high quality SiV ensembles with high optical density to achieve state-of-the-art high bandwidth optical quantum memories. Growth of this material has been achieved through a NIRIM type diamond reactor, (figured top right). Diamond growths have been conducted (figured bottom right) under varying conditions to find the parameters for single crystal diamond growth. The reactor is based on a space constrained design [4] and modified for higher vacuum to ensure an extremely low leak rate to



achieve very high sample purity. Varying Si/C ratios are currently being studied to find optimized conditions for high quality material and sufficient absorption by the SiV. In this poster, I will introduce the properties of the SiV and the potential of in-situ silicon doping during CVD.



- [1] J. P. Dowling and G.J. Milburn, Philos. Trans. R. Soc. A **361**, 1655 (2003).
- [2] J. N. Becker, Ph.D. Thesis, Saarland University (2017).
- [3] C. Weinzetl, et al., Phys. Rev. Lett. 122, 063601 (2019).
- [4] E. H. Thomas et al., AIP Adv. 8, 035325 (2018).

Impact of Ionospheric Mesoscale Flow Enhancements on Polar Cap Patch Propagation

<u>Amelia Lee</u> ^a, Toshi Nishimura ^b, Katherine Davidson ^b, Waqar Younas ^b, Tuija Pulkkinen ^a, Nozomu Nishitani ^c and Kazuo Shiokawa ^c

(a) Climate and Space Science and Engineering, University of Michigan (ameliale@umich.edu)
(b) Center for Space Physics, Boston University (toshi@bu.edu)
(c) Nagoya University (nisitani@isee.nagoya-u.ac.jp)

The ionosphere-thermosphere system is a highly dynamic region impacted by large- and meso-scale drivers. Polar cap patches are dense regions of plasma in the F-region ionosphere at least twice as dense as surrounding plasma [1]. On a large-scale, polar cap patch behavior and propagation is generally understood to follow the large-scale anti-sunward plasma convection in a southward IMF [2]. Although meso-scale plasma convection is known to exist within the large-scale patterns, their evolution and impact on the patches are not as well understood. Characterizing the lifetime, structure, and effect of mesoscale ionospheric flows will provide context as to how they might impact and/or drive polar cap patch propagation and evolution.

In this study, we present two case studies that highlight the evolution of polar cap patches in relation to meso-scale ionospheric flow structures using 630.0 nm optical data from the OMTI All-Sky-Imager located at Eureka and Resolute Bay, Canada, and high-resolution convection maps from SuperDARN. We found that, within the large-scale ionospheric flow pattern, when meso-scale flow channels are co-located with the polar cap patches, they change the flow direction and speed of the polar cap patches. These mesoscale flow channels change on a smaller spatial and temporal scales than the large-scale ionospheric flows. The polar cap patches respond to changes in the direction and strength of the mesoscale flow channels contained in the large-scale ionosphere flow patterns, often slowing down soon after the mesoscale flows cease or changing direction as other flow channels appear. These results show that polar cap flows often involve meso-scale flow channels, and that polar cap patch behavior is closely tied to mesoscale flow channels.

References

[1] Crowley G. 1996. Critical review on ionospheric patches and blobs. In: Review of radio science, 1992–1996, Stone WR (Ed.), Oxford Univ. Press, New York, NY, pp. 619.

[2] Lyons, L. R., Y. Nishimura, and Y. Zou (2016), Unsolved problems: Mesoscale polar cap flow channels' structure, propagation, and effects on space weather disturbances, J. Geophys. Res. Space Physics, 121, 3347–3352, doi:10.1002/2016JA022437.

Molecular Dynamics Simulations of Temperature Relaxation in Strongly Magnetized, Antiproton-Electron Plasmas*

James C. Welch III a, Louis Jose, Timothy D. Tharp b and Scott D. Baalrud a

- (a) Nuclear Engineering & Radiological Sciences, University of Michigan, Ann Arbor, Michigan 48109, USA (welchjc@umich.edu)
 - (b) Physics, Marquette University, Milwaukee, Wisconsin, 53233, USA

Cooling antiprotons is a vital step in the synthesis of antihydrogen. This is achieved via collisional relaxation with electrons that are cooled by cyclotron emission in a Penning-Malmberg trap [1]. These traps present a novel plasma physics regime as the particles are strongly magnetized in the sense that the gyroradius exceeds the plasma frequency. A recent model [2] describing the temperature evolution under these conditions predicts temperatures parallel to the magnetic field equilibrate much faster than perpendicular to it. Here, molecular dynamics simulations are used to test this model and its predictions. Two analysis methods are employed. The first is based on an applied temperature difference that is allowed to relax. The second employs a novel Green-Kubo relation to extract relaxation rates from equilibrium temperature fluctuations. The simulation results support the predictions of the model.

* NSF grant award No. PHY-2205506

- [1] J. Fajans and C. Surko, Physics of Plasmas 27, 030601 (2020).
- [2] L. Jose, J. C. Welch III, T. D. Tharp, and S. D. Baalrud, Physical Review E 111, 035201 (2025).

Two-Frequency RF Fields Induced Multipactor in Coaxial Transmission Line* Md Mashrafi ^a, Asif Iqbal ^a, John Verboncoeur ^b and Peng Zhang ^a

- (a) Department of Nuclear Engineering and Radiological Sciences, University of Michigan, Ann Arbor, Michigan 48109, USA (mdmash@umich.edu)
- (b) Department of Computational Mathematics, Science, and Engineering, Michigan State University, East Lansing, Michigan 48824-1226, USA

This work investigates multipactor discharge in coaxial geometry [1] with two-frequency rf electric field $[\sin(\omega t + \theta) + \beta \sin(n(\omega t + \theta) + \gamma)],$ where V_{rf} is the peak voltage, β is the field strength of the second carrier mode relative to fundamental mode, n is the ratio of two carrier frequencies and γ is the relative phase of second carrier mode. We that multipactor susceptibility depends strongly on β and γ , using Monte Carlo simulations [2,3]. In Figure 1(a), a single-frequency drive with aspect ratio $\frac{b}{a} = 2$ produces a broad multipactorsusceptible band across $f \times d$, with the multipactor threshold voltage rising with frequency. Increasing the aspect ratio to $\frac{b}{a} = 5$ reshapes and shrinks this band, as shown in Figure 1(b). By keeping the geometry fixed at $\frac{b}{a} = 2$, but switching to a two-frequency drive in Figure 1(c) (n=2; $\beta = 1$; $\gamma = \frac{3\pi}{2}$) also contracts the region. susceptible Overall, both geometric change (larger b/a) and twofrequency drive influence the multipactor susceptibility chart and consequently, the multipactor threshold.

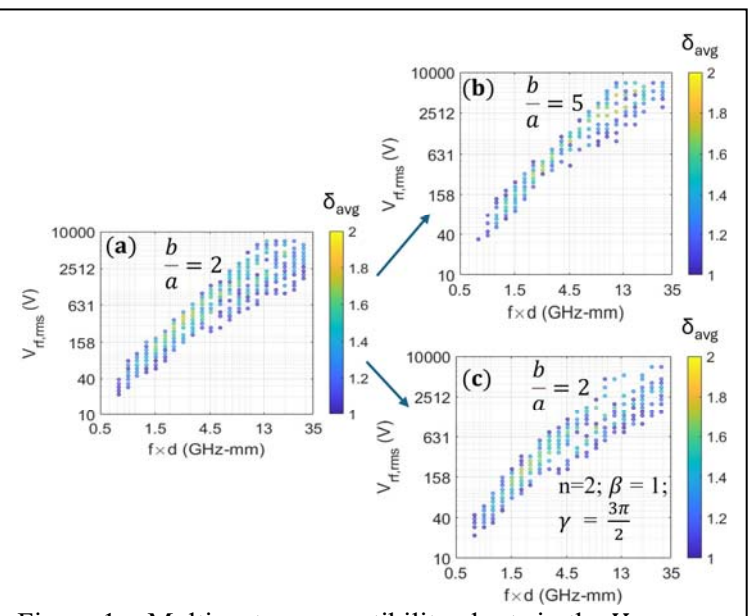


Figure 1 – Multipactor susceptibility charts in the $V_{rf,rms}$ – fd space calculated from Monte Carlo (MC) simulations with image-charge effects for (a) –(b) single frequency rf operation for aspect ratio $\frac{b}{a}=2$ and $\frac{b}{a}=5$ respectively, (c) two-frequency rf operations with aspect ratio $\frac{b}{a}=2$, relative phase of the second carrier $\gamma=3\pi/2$, relative strength of the second carrier $\beta=1$ and frequency ratio between the two carrier modes n=2. Here, $V_{rf,rms}=V_{rf}/\sqrt{2}$ is the rms voltage of rf fields, f is the fundamental frequency and d is the gap distance. δ_{avg} is the average value of the secondary electron yield over 50 impacts in the coaxial line.

*Work supported by the Air Force Office of Scientific Research (AFOSR) MURI through Grant Numbers FA9550-18-1-0062, FA9550-21-1-0367, and FA9550-20-1-0409, and from Department of Energy (DOE) Basic Energy Sciences (BES) Award DE-SC0026271.

- [1] J. R. M. Vaughan, IEEE Trans. Electron Devices 35, no. 7, pp. 1172–1180 (1988).
- [2] A. Iqbal, Phys. Plasmas 29, no. 1, (2022).
- [3] A. Iqbal, High Volt. **8**, no. 6, pp. 1095–1114, (2023).

Do Mercury's Dipolarization Fronts Originate from Flux Ropes? MHD-AEPIC Simulations of Mercury's Magnetosphere*

Alexander T. Cushen ^a, Xianzhe Jia ^a, James Slavin ^a, Weijie Sun ^b,

Gabor Toth a, and Yuxi Chen a

(a) Department of Climate and Space Sciences, University of Michigan (atcushen@umich.edu)
(b) Space Sciences Laboratory, University of California, Berkeley

Mercury's small magnetosphere and strong solar wind driving result in short-lived, highly dynamic substorms where large amounts of magnetic flux is processed in the magnetotail through nightside reconnection. This processing is realized through the rapid formation of planetward and tailward-moving flux ropes (FRs) and dipolarization fronts (DFs), which heat the plasma sheet near the planet and interrupt the duskward cross-tail current. The MESSENGER spacecraft observed DFs

and FRs during its orbital campaign from 2011-2015, but open questions about their dynamics, relationship to each other, and role in broader magnetospheric processes persist.

To contextualize these observations, we present coupled fluid-kinetic simulations of Mercury's magnetosphere using the MHD-AEPIC code implemented through the Space Weather Modeling Framework. This model utilizes a Hall-MHD solver for the global magnetosphere coupled to an embedded particle-in-cell code, which simulates the magnetotail dynamics. By tracking the time-resolved propagation of the DFs, we find that a minority of events originate through direct single x-line reconnection, while the majority originate from flux ropes formed further down the tail that

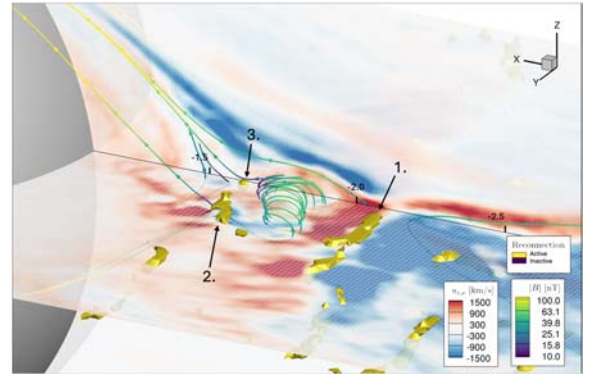


Figure 1 - 3D view of Mercury's magnetotail from MHD-AEPIC simulation, showing fast planetward flows (red), with an embedded flux rope (colored streamlines). The flux rope is fed by reconnection site (1), at the same time that is dissipating at site (2).

undergo secondary reconnection closer to the planet to create DF-like signatures.

We probe the distribution of these features in the current sheet, showing how a dominant dawnward drift emerges independent of dawn-dusk reconnection site asymmetries. We investigate the different energy transfer processes between DFs and FRs, highlighting phenomenological signatures in their evolution and bulk particle properties which could help to distinguish them observationally. FRs are found to ``re-reconnect" with the planetary dipole field, energizing the plasma along the reconnecting flux tube and forming a substorm current wedgelet. This observation allows us to trace their impact on the formation and maintenance of long-lived dipolarization regions, where Mercury's magnetic field is enhanced above dipole levels at low altitudes for substorm timescales.

^{*} Work supported by NASA FINESST program through grant #80NSSC24K1707.343.

Molecular Dynamics Simulations of Electrical Conductivity in Strongly Magnetized Plasmas*

Kyle Kemmerer, Louis Jose and Scott D. Baalrud

Department of Nuclear Engineering & Radiological Sciences, University of Michigan, Ann Arbor, MI (kylekem@umich.edu)

Understanding transport processes in strongly magnetized plasmas is critical for accurate magnetohydrodynamic (MHD) modeling of systems ranging from Z-pinch experiments to non-neutral and ultracold neutral plasmas. These strongly magnetized plasmas are characterized by gyrofrequencies exceeding the plasma frequency, corresponding to magnetization parameter $\beta = \omega_c/\omega_p > 1$ [1].

Electrical conductivity, one transport coefficient, is well described by traditional plasma kinetic theories in weakly magnetized regimes. However, these theories fail when plasma becomes strongly magnetized. As such, here we use two-species molecular dynamics (MD) simulations to study the electrical conductivity of strongly magnetized electron-ion plasmas. With no theory applicable to these strongly magnetized conditions, MD simulations provide a first-principles

method to explore new regimes and serve as a benchmark for future theories. Our results show that the electrical conductivities parallel and perpendicular to the magnetic field initially decrease and separate with increasing β , but surprisingly both plateau at even higher magnetization.

The MD Simulations were performed using the open-source MD software LAMMPS, and Green-Kubo relations were used to obtain the conductivity from the particle velocities. In addition to studying the effects magnetization, the work also examines how Coulomb coupling (Γ) , in conjunction with magnetization, strong affects electrical conductivity. Here, the Coulomb coupling parameter Γ is the ratio of potential energy at the average interparticle spacing to the average kinetic energy of the plasma. A kinetic theory is also being developed to help explain the observed trend.

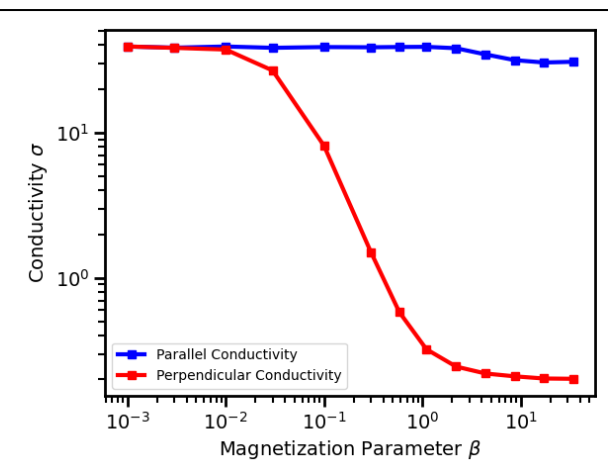


Figure 1 – MD simulation results for plasma conductivity parallel (blue) and perpendicular (red) to the magnetic field at $\Gamma=0.1$ as a function of magnetization parameter. Perpendicular conductivity falls away from the parallel first before the parallel follows less dramatically, with both finally plateauing at even higher magnetization.

References

[1] S. D. Baalrud and J. Daligault, Physical Review E **96**, 043202 (2017).

^{*} This material is based upon work supported by NSF Grant Award No. PHY-2512424

Homogeneous vs. Plasma Chemistry in High Temperature Methane DBDs: A Global Kinetic and Graph Theory Analysis

<u>Ibukunoluwa Akintola</u> ^a, Mikhail Vasilev ^a, and David B. Go ^{a,b}

- (a) Department of Aerospace and Mechanical Engineering, University of Notre Dame, IN 466556
- (b) Department of Chemical and Biomolecular Engineering, University of Notre Dame, IN 46556

Non-thermal plasma offers a compelling pathway for transforming methane (CH₄) into higher-value chemical products, providing an alternative approach for utilizing natural gas and related feedstocks. Prior investigations have revealed that CH₄ conversion efficiency within dielectric barrier discharge (DBD) reactors strongly depends on the bulk gas temperature, with CH₄ conversion inhibition occurring at temperatures exceeding 600 °C. To optimize performance and reactor design, it is essential to understand how plasma-driven and thermally driven processes interact under these elevated conditions. In this study, a ZDPlasKin kinetic modeling framework was employed to analyze how gas-phase effluent composition evolves with temperature in both pure CH₄ and CH₄/argon (Ar) DBD plasmas, consistent with previous experimental observations. Kinetic simulation data were used to construct reaction networks, in which species were represented as nodes and reaction rates defined the edge weights. To reduce the complexity of these networks, edge betweenness centrality (EBC) analysis was applied to identify key reactions governing chemical pathway shifts at higher temperatures. The analysis revealed that the product distribution and dominant reaction routes vary with temperature. Elevated temperatures enhance pathways that promote CH₄ reformation, suppressing overall conversion by altering chain propagation and termination reactions. These findings indicate that temperature-induced changes in homogeneous thermal chemistry, rather than modifications to plasma behavior itself, are primarily responsible for the observed conversion inhibition in high-temperature DBD plasmas.

Abstracts: Poster Session II

Interface-preserving Numerical Methods for Radiation Hydrodynamics W. Curtis Maxon ^a, Joshua Dolence ^b, Jonah Miller ^b, Karthik Duraisamy ^a, Eric Johnsen ^a

(a) University of Michigan(b) Los Alamos National Laboratory

Robust simulation of multi-physics phenomena, such as those found in experiments at the National Ignition Facility, require foundational numerical methods to model accurately. The design process is necessarily enhanced by the use of these numerical simulations due to the high cost of the experiments. This work addresses a challenge in numerical radiation-hydrodynamics in the infinite limit of opacity and perfect isotropy: spurious pressure wave generation at material interfaces. Even without interfacial perturbations or driving forces, non-physical pressure waves can emerge at material interfaces and propagate throughout the domain. For applications like Rayleigh-Taylor Instability studies—where small perturbations can dramatically alter system evolution—these artifacts compromise solution fidelity and limit the method's utility for more complex multi-material, multi-physics simulations. We implement an interface-preserving criterion based on Abgrall's 1996 approach, adapted for the simplified radiation-hydrodynamics equations [1]. This capability provides the numerical foundation necessary for accurate multi-physics simulations involving complex material interactions, shock-interface coupling, and other phenomena critical to inertial confinement fusion and astrophysics applications.

* This work was supported by Los Alamos National Laboratories (LANL) under the project "Algorithm/Software/Hardware Co-design for High Energy Density applications" at the University of Michigan and the M3AP project under the Advanced Scientific Computing program at LANL.

References

[1] Abgrall, Rémi. "How to prevent pressure oscillations in multicomponent flow calculations: a quasi conservative approach." Journal of Computational Physics **125**.1 (1996): 150-160.

Zero-Dimensional Plasma-Catalysis Model for Surface Coverage of Nitrogen and Oxygen Atoms

Wencheng Lin, Sankhadeep Basu and Hongtao Zhong

Department of Mechanical Engineering, Michigan State University, East Lansing, MI, US, 48824 (linwenc1@msu.edu, hongtaoz@msu.edu)

Non-equilibrium generation of atomic species on the catalytical surface is critical to plasma applications in chemical manufaccturing and processing. Recent experimental measurements by XPS [1] have shown plasma catalysis is efficient for nitrogen and oxygen adsorption under atmospheric pressures. However, little is known about the surface chemical mechanisms and the role of the intermediate surface species. As a result, the design of plasma-catalysis systems has largely relied on empirical trial-and-error approaches, highlighting the need for predictive reaction models.

In this work, an elementary surfacereaction model is developed which considers a nitrogen and oxygen mixture involving atomic nitrogen, atomic oxygen, vibrationally excited and electronically excited species. We analyzed the surface coverage and validated the model with existing experimental data [2]. The model shows there is a competition of atomic O and atomic N for occupying the surface sites and the surface chemistry transits from the Eley-Rideal (E-R) reaction, Langmuir–Hinshelwood (L-H) reaction, to desorption-limited reaction when the pressure is varied. The ongoing work includes coupling this surface chemistry model to the zero-dimensional gas phase plasmachemistry solver [3] and multi-dimensional

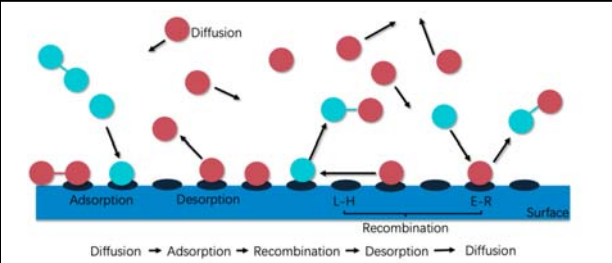


Figure 1 - Schematic illustration of heterogeneous surface recombination processes for nitrogen and oxygen atoms. Gas-phase species diffuse from the boundary layer toward the catalytic surface, undergo adsorption, surface diffusion, and recombination through the Langmuir–Hinshelwood (L–H) or Eley–Rideal (E–R) mechanisms, and subsequently desorb as diatomic molecules.

fluid-based model [4]. The ultimate objective is to have a first-principles-guided predictive model for calculating the surface coverage for plasma catalysis.

* This work is supported by Michigan State University faculty startup and the Princeton Collaborative Low Temperature Plasma Research Facility (PCRF).

- [1] Zhong, H., Piriaei, D., Liccardo, G., Kang, J., Wang, B., Cargnello, M., & Cappelli, M. A. (2025). Cold plasma activated CO₂ desorption from calcium carbonate for carbon capture. RSC Sustainability, 3(2), 973-982.
- [2] Rutigliano, M., & Cacciatore, M. (2016). Recombination of oxygen atoms on silica surface: new and more accurate results. Journal of Thermophysics and Heat Transfer, 30(1), 247-250.
- [3] Zhong, H., Mao, X., Rousso, A. C., Patrick, C. L., Yan, C., Xu, W., ... & Ju, Y. (2021). Kinetic study of plasma-assisted n-dodecane/O₂/N₂ pyrolysis and oxidation in a nanosecond-pulsed discharge. Proceedings of the Combustion Institute, 38(4), 6521-6531.
- [4] Mao, X., Zhong, H., Zhang, T., Starikovskiy, A., & Ju, Y. (2022). Modeling of the effects of non-equilibrium excitation and electrode geometry on H2/air ignition in a nanosecond plasma discharge. Combustion and Flame, 240, 112046.

Harnessing Ionization Effects for Direct Laser Acceleration of Electrons*

<u>Nicolas Kalem</u> ^a, Veronica Contreras ^b, Alexey V. Arefiev ^c, Jessica Shaw ^d, Hui Chen ^e, Félicie Albert ^f, and Louise Willingale ^g

- (a) University of Michigan, Ann Arbor, MI (nmontyk@umich.edu)
- (b) University of Michigan, Ann Arbor, MI (nmontyk@umich.edu)
- (c) University of California, San Diego, CA (aarefiev@ucsd.edu)
- (d) Laboratory for Laser Energetics, Rochester, NY (jshaw05@lle.rochester.edu)
 - (e) Lawrence Livermore National Lab, CA (chen33@llnl.gov)
 - (f) Lawrence Livermore National Lab, CA (albert6@llnl.gov)
 - (g) University of Michigan, Ann Arbor, MI (wlouise@umich.edul)

Direct laser acceleration (DLA) may efficiently accelerate high-energy electron beams when a high-intensity short-pulse laser propagates through an underdense plasma, thereby creating a charge density channel. In this research, we investigate the effect of ionization on the DLA. Typically, helium is used as the target gas due to its relatively low ionization threshold; helium gas is fully ionized by the laser pre-pulse at intensities that are orders of magnitude lower than the pulse peak. By doping the target with heavier gases that fully ionize near the peak intensity, electrons are ionized within a developing channel in which the laser can accelerate them more effectively. Thus, a higher signal and more energetic yield of electrons, and by extension betatron X-rays, may be obtained. This is similar to a method developed to enhance the electron beam charge from laser-wakefield acceleration. Experiments were performed at the OMEGA-EP facility where different gas targets with helium, nitrogen, and argon were tested at varying densities. The experimental results exhibit an elevated electron and X-ray signal that is dependent on the gas density and mixture. Additionally, we use particle-in-cell simulations to further explore this parameter space.

* The experiment was conducted at the Omega Laser Facility with the beam time through the National Laser Users' Facility user program. This material is based upon work supported by the Department of Energy [National Nuclear Security Administration] University of Rochester "National Inertial Confinement Fusion Program" under Award Number(s) DE-NA0004144 and the U. S. Department of Energy under Award DE-SC00215057. This material is based upon work supported by the Department of Energy National Nuclear Security Administration under Award Number DE-NA0004203. The authors would like to acknowledge the OSIRIS Consortium, consisting of UCLA and IST (Lisbon, Portugal) for providing access to the OSIRIS 4.0 framework. Work supported by NSF ACI-1339893.

Effect of a Rectangular Bias Waveform on Cryogenic Plasma Etching of SiO₂*

Yeon Geun Yook ^a, Chenyao Huang ^b, Yifan Gui ^c and Mark J. Kushner ^a

- (a) Department of Electrical Engineering and Computer Science, University of Michigan (ygyook@umich.edu, mjkush@umich.edu)
- (b) Department of Chemical Engineering, University of Michigan (chenyaoh@umich.edu)
- (c) Department of Nuclear Engineering & Radiological Sciences, University of Michigan (evangyf@umich.edu)

The scaling limitations of semiconductor fabrication have shifted device design from lateral shrinkage to vertical stacking, requiring the etching of high aspect ratio (HAR) structures exceeding 100. Increasing aspect ratio introduces severe bowing and aspect ratio dependent etching (ARDE) effects, which remain major challenges. Cryogenic plasma operated substrate etching (CPE). at temperatures between -100 and 0 °C, has emerged as an effective alternative to conventional etching, enabling fast and vertical HAR etching of dielectrics such as SiO₂ through HF-H₂O co-adsorption.

To further enhance CPE performance, a rectangular bias (RB) waveform is introduced. Compared with the conventional sinusoidal radio frequency (RF) bias, the RB waveform

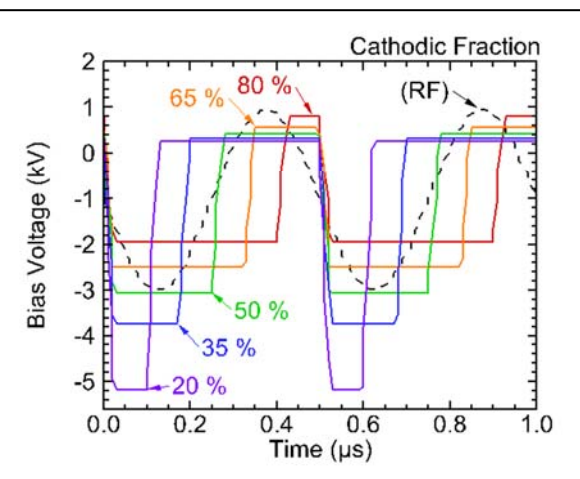


Figure 1 - Comparison of voltage waveforms for both the radio frequency (RF) and tailored rectangular bias (RB) operated at 2 MHz and 2,500 W. The cathodic fraction (CF) of the RB waveform is varied from 20 % to 80 %.

sustains a negative peak voltage for longer within each cycle, providing more efficient ion acceleration and better control of the ion energy and angular distributions (IEADs).

In this study, computational investigations were performed using the Hybrid Plasma Equipment Model (HPEM) and the Monte Carlo Feature Profile Model (MCFPM) to analyze CPE of SiO₂ at both reactor and feature scales. Under identical average power conditions, the plasma properties and resulting feature profiles were compared between RF and RB bias waveforms. The cathodic fraction (CF), defined as the portion of the RB cycle sustaining the negative peak voltage, was varied to examine its impact on IEADs and etch profiles. Excessively high CF narrowed the IEADs but reduced the maximum ion energy, leading to bowed profiles, whereas too low CF caused profile degradation due to insufficient ion acceleration. In addition, variations in CF reduced sidewall charge build-up, one of the causes of profile tilting and twisting, compared to the RF bias. An optimal CF value was identified, where the RB waveform produced more favorable IEADs and improved charge dissipation than the RF bias. These results suggest that the optimized RB waveform can open the possibility for realizing HAR structures in CPE.

* Work supported by Samsung Electronics.

- [1] A. Agarwal and M. J. Kushner, Journal of Vacuum Science & Technology A 23, 1440 (2005).
- [2] X. Shi, S. Sadighi, S. Rauf, H. Luo, J.-C. Wang, J. Kenney, J.-P. Booth, D. Marinov, M. Foucher and N. Sirse, Journal of Vacuum Science & Technology A 43, 13001 (2025).

Anisotropic Charge Transport and Current Crowding in Vertical Thin-Film Contacts with 2D Layered Materials

Md Arifuzzaman Faisal and Peng Zhang

Department of Nuclear Engineering and Radiological Sciences, University of Michigan, Ann Arbor, Michigan, 48109-2104, USA (e-mail: faisalmd@umich.edu).

Electrical [1] layered contacts to semiconductors and 2D materials often struggle with current crowding and high spreading (constriction) resistance due to their highly anisotropic transport properties. In layered van der Waals materials, carriers move much more easily in-plane than out-of-plane, often by factors conductivity anisotropy of exceeding a thousand [2]. Conventional models for calculating spreading resistance typically assume isotropic transport [3], which may result in inaccurate extraction of intrinsic parameters. We present an exact analytical framework based on the conductivity-tensor form of the Laplace equation. $(\nabla \cdot (\boldsymbol{\sigma} \nabla \Phi) = 0),$ which incorporates both in-plane and out-of-plane resistivities, interfacial resistivity, and finite geometry in planar and cylindrical contact configurations. The solutions

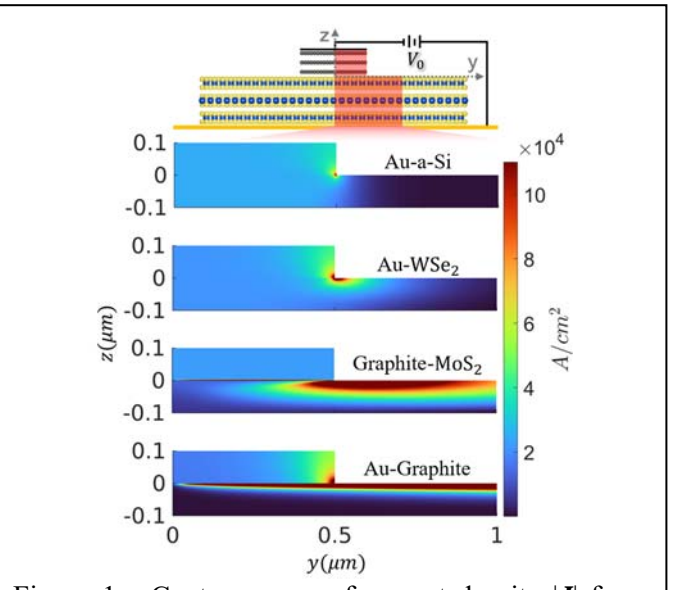


Figure 1 - Contour maps of current density |J| from exact field solutions for four configurations: isotropic (Au-a-Si), moderately anisotropic bottom layer (Au-WSe₂), both anisotropic layers (graphite-MoS₂) and strongly anisotropic bottom (Au-graphite).

uncover that strong in-plane conductivity in MoS₂, WSe₂, and graphite drives lateral potential spreading, enhanced edge crowding, and increased spreading resistance. Our model quantitatively recovers the diffusive limit for thick [4,5], wide substrates while exposing its failure for ultrathin films and short channels. Comparisons with finite-element simulations and experimental data on graphite [4] and MoS₂ [5] confirm the theory. This unified framework provides a robust, physics-based tool for designing and optimizing vertical contacts in 2D materials and van der Waals heterostructures.

* The work is supported by the Air Force Office of Scientific Research (AFOSR) Award Nos. FA9550-22-1-0523 and FA9550-20-1-0409.

- [1] Banerjee, S., Luginsland, J. & Zhang, P. Interface Engineering of Electrical Contacts. Phys. Rev. Appl. 15, 064048 (2021).
- [2] Siao, M. D. et al. Two-dimensional electronic transport and surface electron accumulation in MoS2. Nat Commun 9, 1442 (2018).
- [3] Zhang, P. & Lau, Y. Y. Constriction Resistance and Current Crowding in Vertical Thin Film Contact. IEEE Journal of the Electron Devices Society 1, 83–90 (2013).
- [4] Koren, E., Knoll, A. W., Lörtscher, E. & Duerig, U. Meso-scale measurement of the electrical spreading resistance in highly anisotropic media. Appl. Phys. Lett. **105**, 123112 (2014).
- [5] Vijayan, G., Uzhansky, M. & Koren, E. Spreading resistance and conductance anisotropy in multilayer MoS2. Applied Physics Letters **124**, 133101 (2024).

Molecular Dynamics Simulation of Hydrodynamic Transport Coefficients in Plasmas*

Briggs Damman, Jarett LeVan, and Scott D Baalrud

Nuclear Engineering & Radiological Sciences, University of Michigan, Ann Arbor, Michigan 48109, USA

Molecular dynamics (MD) simulations are used to calculate transport coefficients in a twocomponent plasma interacting through a repulsive Coulomb potential. The thermal conductivity, electrical conductivity, electrothermal coefficient, thermoelectric coefficient, and shear viscosity

are computed using the Green-Kubo formalism over a broad range of Coulomb coupling strength, $0.01 \le \Gamma \le 140$.[1] **Emphasis** placed on testing standard results of the Chapman-Enskog solution in the weakly coupled regime ($\Gamma \ll 1$) using these first-principles simulations. As expected, the results show good agreement for $\Gamma \lesssim 0.5$. However, this agreement is only possible if careful attention is paid to the definitions of linear constitutive relations in each of the theoretical models, a point that is often overlooked. For example, the standard Green-Kubo expression for thermal conductivity is a linear combination of thermal conductivity, electrothermal and thermoelectric coefficients computed in the Chapman-Enskog formalism. Meaningful results for electrical conductivity are obtained over the full range of coupling strengths explored, but it is shown that potential and virial

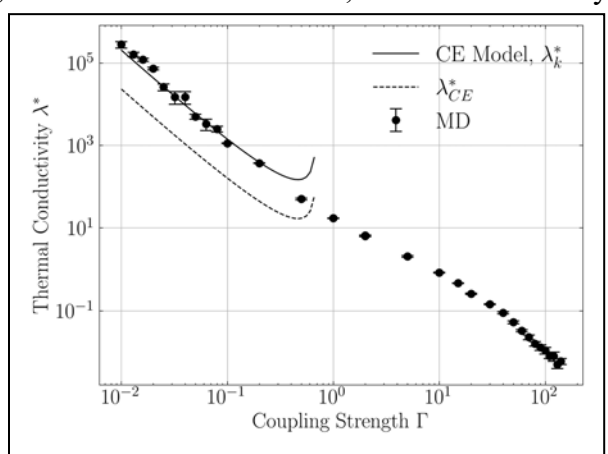


Figure 1 – The kinetic thermal conductivity MD data plotted as a function of Γ . The modified kinetic theory relations (solid line), and traditional definitions (dashed line) are also plotted.

components of the other transport coefficients diverge in the strongly coupled regime ($\Gamma \gg 1$). In this regime, only the kinetic components of the transport coefficients are meaningful for a classical plasma.

* Work was supported by NSF grant no. PHY-2205506.

References

[1] Jarett LeVan, Scott D. Baalrud; Foundations of magnetohydrodynamics. Phys. Plasmas 1 July 2025; 32 (7): 070901. https://doi.org/10.1063/5.0274784.

Model Based Investigation of Self-Consistent Closure in a Hall Thruster Model

Declan Brick, Parker Roberts and Benjamin Jorns

University of Michigan, Department of Aerospace Engineering (brickd@umich.edu)

Anomalous transport in Hall thrusters has been a long standing problem in the electric propulsion community. To account for this issue, Hall thruster models have included an effective "anomalous" collision frequency, but no form has correctly predicted changes in performance with changes in operation. A key challenge in finding a predictive closure is that axial profiles of empirical frequencies have a local reduction by multiple orders of magnitude in order to reproduce the experimentally observed steep electric field profiles. As none of the bulk plasma properties exhibit such a drastic change, it is difficult to capture this variation and correctly place it when the collision frequency is implemented self-consistently. With that said, recent experimental and modeling work

have shed light on a potential path forward. Non-invasive measurements of electron properties have unexpectedly revealed electron temperatures twice as large as previously predicted and magnetic field lines that are non-isothermal [1]. In previous work, we have found that when the electron heat flux is varied, a self-consistently implemente a closure based on the electron-ion collision frequency, can successfully place the peak electric field to within a scaling coefficient [2]. However, the model under predicted the observed peak temperatures and performance metrics and was not fully predictive [2]. Using measured values of the anomalous collision

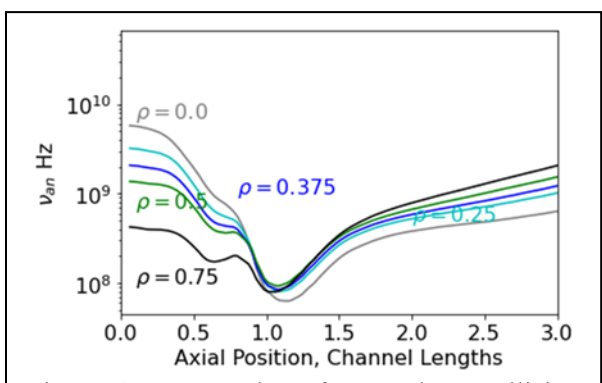


Figure 1 – Examples of anomalous collision frequency in this work for the H9 Hall thruster operating on krypton at 300V and 15A.

frequency, we found that by setting the heat flux along field lines to adiabatic, we can match multiple plasma properties [3]. Using this representation and building on the electron-ion collision frequency in this work we explore the closure

$$v_{an} = 2.9 \times 10^{-12} \text{cln} (\Lambda) \frac{n_e^{\mu}}{n_n^{\rho} T_e^{\tau}}$$

where v_{an} is the anomalous collision frequency, c, μ , τ , and ρ are tunable constants, n_e is plasma density, T_e is electron temperature, and n_n is neutral density. We evaluate model results compared to experimental data of a 9kW class magnetically-shielded Hall thruster to match plasma properties. We then analyze these results to better understand of electron transport in Hall thrusters.

* This work was supported by the Graduate Research Fellowship Program from the National Science Foundation and the NASA Joint Advanced Propulsion Institute. Additional support in part through computational resources and services provided by Advanced Research Computing, a division of Information and Technology Services at the University of Michigan, Ann Arbor.

- [1] P.J. Roberts et. Al, IEPC 393, 38th international electric propulsion conference (2024).
- [2] D.G. Brick, P.J. Roberts, and B.A. Jorns, 298, SciTech 2025 (2025).
- [3] Brick, D., Roberts, P., and Jorns, B., "On the Adiabatic Nature of Electron Energy Transport Along Magnetic Field Lines in Hall Thrusters," In preparation.

Effects of Europa's Atmosphere on Its Magnetic and Plasma Environment: Application of Multi-Fluid MHD Simulations to Spacecraft Flybys

Mitchell Indek and Xianzhe Jia

University of Michigan (mindek@umich.edu)

Observations of Jupiter's moon Europa from in situ spacecraft (e.g., Galileo and Juno) and telescopes (e.g., HST and JWST) have revealed a complex interaction between the moon's tenuous oxygen atmosphere and the ambient Jovian magnetosphere in which it is immersed. The Alfvén wings created by this interaction produce significant perturbations in both the magnetic field and plasma immediately surrounding the moon. Further complicating this interaction is the fact that Europa's atmosphere is highly variable in space and in time, which can change the nature of the interaction by changing the obstacle that Europa effectively presents to the incoming plasma flow, altering the distribution and strength of magnetic perturbations. In this work, we use the BATS-R-US multi-fluid MHD model to simulate the plasma interaction at Europa, systematically varying the parameters controlling the neutral atmosphere profile to explore the effects each of them has on the resulting magnetic and plasma environment around the moon. The variables we examine include atmospheric scale height, surface density, and the placement and size of inhomogeneities. To test how a spacecraft passing by Europa might observe the effects of these atmospheric conditions, we look to apply this approach to the Galileo E4 and E15 flybys. Both flybys took place in Europa's plasma wake but at different Jovian local times and latitudes relative to Jupiter's central plasma sheet, creating conditions where understanding the configuration of the atmosphere is necessary to obtain high-fidelity simulations consistent with observations. Through exploring different kinds of neutral atmosphere models, we seek to identify atmospheric conditions for each of these flybys that provide reasonable agreement to the observed magnetic field and plasma density. Developing the intuition for how Europa's changing atmosphere affects the moon's magnetic and plasma environment will be crucial to the success of both NASA's Europa Clipper mission and ESA's Juice mission, both of which are slated to arrive in the Jovian system in the early 2030s. This is because the characterization of Europa's subsurface ocean and evaluation of its potential habitability relies crucially on measurements of the induced magnetic field Europa's ocean generates in response to Jupiter's time-varying magnetic field, which can be obscured by the magnetic perturbations created by the plasma interaction examined in this work. Therefore, being able to understand and quantify the effects of Europa's atmosphere-plasma interaction will greatly improve the science return of both missions.

Space Plasma Dynamics and the Resulting Energy Flux into Earth's Magnetosphere*

Nolan Tribu ^a, Tuija Pulkkinen ^b and Matti Ala-Lahti ^c

- (a) Climate and Space Sciences and Engineering, University of Michigan (ntribu@umich.edu)
- (b) Climate and Space Sciences and Engineering, University of Michigan (tuija@umich.edu)
 - (c) Faculty of Science, University of Helsinki (matti.ala-lahti@helsinki.fi)

We present the initial results from quantifying the energy transfer along Earth's low latitude dayside magnetopause, a boundary between Earth's magnetic field and the incoming solar wind. Many global magnetohydrodynamic (MHD) simulations have demonstrated the importance of the net energy flow at the boundary and relations to magnetic reconnection.[1] For the first time, a comprehensive investigation of the energy flux across the low-latitude dayside magnetopause that is based on analysis in-situ observations will be done using high resolution data from Magnetospheric Multiscale (MMS) mission, and with over 4000 well defined magnetopause crossings.[2] Initial statistical results agree with simulations for well defined Harris sheet-like crossings, with the general energy flux leaving the magnetosphere to the magnetosheath. There is a clear correlation between the magnetopause boundary motion and the energy flux in the regions surrounding the boundary. In a stationary frame this correlation is no longer present, and gives lower energy magnitudes. The resulting energies in this stationary frame are then dependent on smaller plasma kinetic scale interactions, while future work aims to find correlations in energy flux to magnetic reconnection.

* Work Supported by NSF Grant No. 2420675. MA-L and TP also acknowledge the NSF Grant No. 2033563 and NASA Federal Award No. 80NSSC23M0192.

References

[1] Brenner, A., Pulkkinen, T. I., Al Shidi, Q., and Toth, G. (2021), Storm-time Energetics: Energy Transport Across the Magnetopause in a Global MHD Simulation. Front. Astron. Space Sci. 8, 180 [2] Paschmann, G., Haaland, S. E., Phan, T. D., Sonnerup, B. U. Ã., Burch, J. L., Torbert, R. B., Gershman, D. J., Dorelli, J. C., Giles, B. L., Pollock, C., Saito, Y., Lavraud, B., Russell, C. T., Strangeway, R. J., Baumjohann, W., and Fuselier, S. A.: Large-Scale Survey of the Structure of the Dayside Magnetopause by MMS, J. Geophys. Res.-Space, 123, 2018–2033, 2018.

Experimental Demonstration of a Spatial Anti-aliasing Plasma Wave Analysis Technique on Ion Acoustic Turbulence in a Hollow Cathode Plume

Miron Liu and Benjamin Jorns

The flowing plasma environment of many electric propulsion (EP) devices is conducive to the onset and growth of various plasma instabilities. These waves are believed to manifest numerous deleterious effects, including reduced device efficiency and accelerated erosion of critical components [1]. Given that these waves dominate electron and ion dynamics in EP devices, it is important to account for them in models to rigorously assess their impact on device performance and lifetime. However, a comprehensive understanding of these modes has yet to be achieved. This in large part stems from the limitations of current diagnostics which precludes experimental measurement of moderate-length-scale modes with wavelengths between 1 mm and 5 mm. Aliasing effects arising from the finite spacing between wave probe elements impose a lower bound on the

wavelengths that physical probe-based methods can resolve [2]. In contrast, optical techniques for measuring wave properties, such as Coherent Thompson Scattering (CTS), have inherent upper bounds in spectral bandwidth [3]. In light of these outstanding limitations, Liu and Jorns [4] recently validated an anti-aliasing technique that leverages multipoint correlation and Bayesian inference to reconstruct a de-aliased probability distribution function of dispersion. In principle, this diagnostic technique will allow for an expansion of the resolvable wavelength regime and enable the first experimental measurements of moderate-wavelength modes. However, while the anti-aliasing algorithm showed promise, the aforementioned validation effort was purely numerical. There remains a need to provide an extension of the validation campaign to experimental data. The goal of this work is to address this need.

* Work supported by NASA Space Technology Graduate Research Opportunity (NSTGRO) and Rackham Merit Fellowship (RMF).

References

[1] J. D. Frieman, H. K. Kamhawi, P. Y. Peterson, D. A.
Herman, J. H. Gilland, R. R. Hofer, AIAA P&E Forum, (2019).
[2] B. A. Jorns, I. G. Mikellides, and D. M. Goebel, Phys. Rev. 90, 063106 (2014).

[3] S. Tsikata, K. Hara, S. Mazouffre, J. Applied Phys. **130**, 343304, (2009).

[4] M. F. Liu, B.A. Jorns, AIAA SciTech Forum, (2025).

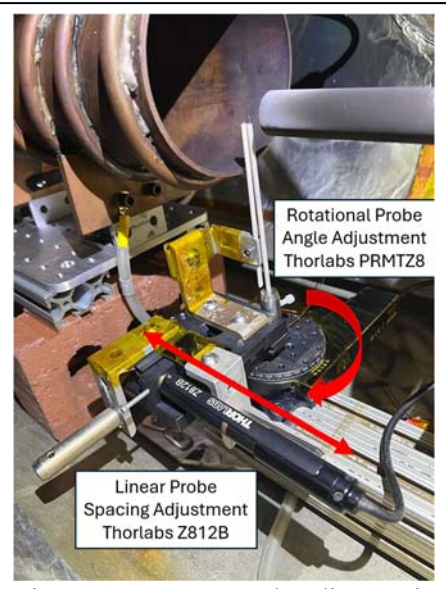


Figure 1 - Wave probe diagnostic for inferring plasma wave dispersion.

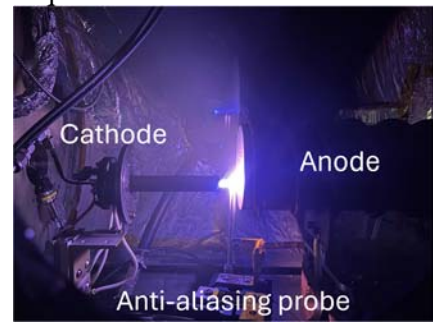


Figure 2 - LaB₆ hollow cathode test article.

Complexity Analysis of a CT Injection Experiment on BRB*

<u>Khalil Bryant</u> ^a, David A. Schaffner ^b, Joseph R. Olson ^c, Karsten J. McCollam ^c, Heath J. LeFevre ^a, Cary Forest ^c and Carolyn C. Kuranz ^a

(a) University of Michigan – Ann Arbor(b) Bryn Mawr College(c) University of Wisconsin - Madison

In this work, we use Jensen-Shannon complexity entropy to analyze the magnetic field fluctuations of an astrophysically-scaled plasma experiment. In the experiment, we used the Big Red Ball (BRB) facility at the University of Wisconsin to create a scaled analog to an interplanetary coronal mass ejection (ICME), scaling according to plasma β , magnetosonic Mach number, and total pressure ratio. Complexity analysis is interesting because, when plotted against each other, complexity and entropy can be used to tell the difference between a chaotic series and a stochastic series. Previous complexity research on ICMEs has concluded that they are highly stochastic. We do similar analysis for the scaled experiment which serves as another way of comparing the experiment with the actual event. In addition to this, we go a step further by investigating complexity as a function of frequency, finding which frequencies maximize complexity. We then compared those frequencies to other frequencies in the plasma, such as the cyclotron frequency and collisional frequencies. We found that the frequencies for maximum complexity do not correspond to the frequencies investigated, implying that there are other physical mechanisms that lead to an increase of complexity at these frequencies.

^{*}This work is funded by the DOE, FES under award DE-SC0021288.

Pulsed Power Strategies for Plasma Etching of High Aspect Ratio Features Using Fluorocarbon Gas Mixture for Feature Charging Control

Yifan Gui, Yeon Geun Yook, Chenyao Huang and Mark J. Kushner

University of Michigan, 1301 Beal Avenue, Ann Arbor, MI 48109-2122, USA (evangyf@umich.edu, ygyook@umich.edu, chenyaoh@umich.edu, mjkush@umich.edu)

In microfabrication, plasma etching of high aspect ratio (HAR) features with precision remains a significant challenge largely due to feature charging effects that can lead to profile distortion and etch stop. Feature charging occurs when there is an imbalance in the flux of ions and electrons to inside surfaces of features, leading to the creation of local electric fields that deflect incoming charged species and distort ion trajectories. Previous experimental and modeling studies have shown the sensitivity of feature charging on energy and angular distributions (EADs) of charges species incident onto the wafer. Potential remedies for feature charging include pulsed plasma operation, tailored bias waveforms, and the introduction of electronegative gases to suppress electron density or promote charge neutralization. These strategies aim to balance ion and electron fluxes or temporarily neutralize accumulated charge to mitigate defects within the HAR features. For example, the use of pulsed power is believed to produce a cycle of charging and discharging of the feature as the fluxes and EADs of the charged particles are modulated.

In this work, we discuss a computational investigation of pulse power strategies for controlling the fluxes of charged particles to wafers in capacitively coupled plasmas (CCPs) with the goal of mitigating feature charging. The Hybrid Plasma Equipment Model (HPEM), a modular simulator designed to address the behavior of low-pressure plasma systems, was used to investigate the evolution of incident fluxes and EADs of charged particles during pulse-on and off periods in multi-frequency CCPs using fluorocarbon gas mixtures and mixtures amenable to cryogenic etching. The consequences of utilizing different modes of pulse operation (low frequency, high frequency, dc) and gas mixtures on the EADs and charged species flux will be discussed in relation to minimizing feature charging.

^{*} Work supported by Lam Research, Samsung Electronics and Department of Energy Office of Fusion Energy Sciences.

Effects of Annular Beam Properties on Gap Coupling in High-Frequency Microwave Devices

Md Wahidur Rahman a and Peng Zhang b

(a) Michigan State University, East Lansing, MI, USA (rahman63@msu.edu)(b) University of Michigan, Ann Arbor, MI, USA (umpeng@umich.edu)

Efficient energy transfer in high-frequency microwave devices depends on strong electron beam-cavity interaction [1]. Solid beam linear devices are often limited in RF power and efficiency

due to limited beam cross-section area and spacecharge effects [2]. In contrast, annular beams are advantageous for mitigating these effects for wideband and high-power applications as to enhance beam—cavity coupling through variations in current density distribution and inner beam radius.

In this work, we analyze the gap coupling factor of an annular beam under large-signal operation using both analytical model and disk model that incorporates space-charge effects. We conduct a systematic parametric scaling analysis for two configurations: first, by maintaining the same total cross-sectional area as a solid beam while varying the inner and outer beam radii; and second, by fixing the outer beam radius while varying the inner beam radius. Our results quantitatively show how increasing the ratio of inner to outer beam radius results in a higher gap coupling factor, lower effective kinetic energy, and

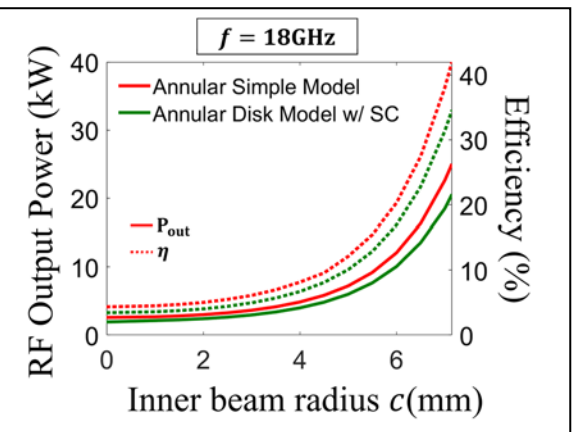


Figure 1 - Comparison of RF output power (solid lines) and efficiency (dotted lines) for a single gap-cavity device for different inner beam radius when outer beam radius b=7.2 mm at f=18GHz (K-band). The results are calculated from large signal simple model and disk model with space charge effects.

improved beam to RF conversion efficiency by modifying the current density and beam cross sectional area [3]. The output power and efficiency of annular beams are significantly higher than those of solid beams at high frequency. These results provide practical design guidelines for annular beam profiles, enabling improved performance and efficiency in next-generation microwave devices.

* This work was supported by the Air Force Office of Scientific Research (AFOSR) Grant No. FA9550-20-1-0409, and the Air Force Office of Scientific Research (AFOSR) Grant No. FA9550-22-1-0523.

- [1] R. G. Carter, Microwave and RF Vacuum Electronic Power Sources, 1st ed. Cambridge University Press, 2018. doi: 10.1017/9780511979231.
- [2] M. W. Rahman and P. Zhang, "Parametric analysis of electron beam—wave interaction in linear beam devices: A tutorial on gap coupling factor and scaling to high frequency," AIP Advances **15**, no. 3, p. 035128, Mar. 2025, doi: 10.1063/5.0254067.
- [3] M. W. Rahman and P. Zhang, "Gap Coupling Factor of an Annular Electron Beam," IEEE Trans. Plasma Sci., pp. 1–6, 2025, doi: 10.1109/TPS.2025.3605560.

Foundations of Magnetohydrodynamics with Applications to Dense Plasmas* Jarett LeVan ^a and Scott Baalrud ^b

(a) Applied Physics, University of Michigan, Ann Arbor, MI (jarettl@umich.edu)
(b) Nuclear Engineering & Radiological Sciences (baalrud@umich.edu)

A derivation of magnetohydrodynamics (MHD) valid beyond the usual ideal gas approximation is presented [1]. Non-equilibrium thermodynamics, a macroscopic framework for describing irreversible processes, is used to obtain conservation equations and linear constitutive relations. When coupled with Maxwell's equations, this provides closed fluid equations in terms of material properties of the plasma, described by the equation of state and transport coefficients. It is then shown how these properties are connected to microscopic dynamics using the Irving-Kirkwood procedure and Green-Kubo relations. Discussions of symmetry arguments and the Onsager-Casimir relations are provided, which allow one to vastly simplify the number of independent coefficients. Importantly, expressions for current density, heat flux, and stress (conventionally Ohm's law, Fourier's law, and Newton's law) take different forms in systems with a non-ideal equation of state. The traditional form of the MHD equations, which is usually obtained from a Chapman-Enskog solution of the Boltzmann equation, corresponds to the ideal gas limit of the general equations. Moreover, it is shown how the transport coefficients defined in kinetic theory relate to those from the Green-Kubo relations.

* This work was supported by NSF grant no. PHY-2205506 and NNSA grant no. DE-NA0004148.

References

[1] J. Levan and S.D. Baalrud, Physics of Plasmas 32.7 (2025).

Fusing Ground-Based and GOLD Inferred TEC Using Statistical Calibration*

Mary Smirnova, Shasha Zou and Grace Kwon

University of Michigan (margysk@umich.edu)

This study investigates the feasibility of fusing satellite-inferred and ground-based TEC measurements to enhance global ionospheric specification and characterization. The TEC values are derived from the GOLD satellite's 135.6 nm oxygen emission using the methodology of Qin et al. (2023) and are statistically calibrated to account for inherent assumptions in the derivation process. The calibrated GOLD-derived TEC is then integrated with the Madrigal ground-based TEC measurements and used as input for the VISTA model. To improve data integrity, filtering is applied to exclude contamination from solar and polar auroral emissions. Additionally, large-scale background TEC structures are separated from small-scale depletions such as Equatorial Plasma Bubbles (EPBs) by a rolling ball algorithm described by Pradipta et al. (2024), and constructed as a validation dataset for numerical models that do not explicitly incorporate EPB physics. Using the VISTA data based on the fused TEC input, our preliminary results provide new insights into equatorial and midlatitude ionospheric dynamics, such as the hemispheric asymmetry of EIAs. This work underscores the potential of multi-source TEC fusion in advancing our capability of specifying the ionosphere and understanding ionospheric phenomena, such as equatorial plasma bubbles.

* This work is supported by the Space Weather Operational Readiness Development (SWORD) — a NASA Space Weather Center of Excellence under grant 80NSSC23M0192, as well as NASA grants: 80NSSC20K0190, 80NSSC20K1313, 2024GC0698, and NSF grant NSF 2419187.

References

[1] Qin, J., Liu, H., Yin, X., Liu, M., Wang, J., Mao, T., et al. (2023). Inferring the ionospheric state with the far ultraviolet imager on the Fengyun-4C geostationary satellite: Retrieval algorithm and verification. [2] Hu Sun. Zhijun Hua. Jiaen Ren. Shasha Zou. Yuekai Sun. Yang Chen. "Matrix completion methods for the total electron content video reconstruction." Ann. Appl. Stat. 16 (3) 1333 – 1358, September 2022. https://doi.org/10.1214/21-AOAS1541.

Multiscale Modeling of Radical and Vibrational Pathways in Plasma-Assisted Ammonia Synthesis on Fe (110) and Ni (111)*

Oluwatosin A. Ohiro, Samuel A. Ogunwale and Bryan R. Goldsmith

Department of Chemical Engineering, University of Michigan, Ann Arbor, USA (oohiro@umich.edu)

Low-temperature plasma (LTP)-assisted ammonia synthesis is a promising alternative to the Haber-Bosch process for decentralized, renewable energy-driven production. Progress has been limited by an incomplete mechanistic understanding, particularly the debated roles of vibrationally excited $N_{2(g),v}$ and plasma-generated $N\cdot/H\cdot$ radicals, which may explain the unexpected insensitivity of catalyst performance across metals. We apply a multiscale computational framework, combining density functional theory (DFT) modeling and a packed-bed reactor microkinetic model, to

disentangle these contributions to LTP-assisted $NH_{3(g)}$ synthesis over Fe (110) and Ni (111) catalysts. The model incorporates experimentally derived vibrationally excited $N_{2(g),v}$ distributions from an RF plasma and accounts for their vibrational surface quenching.

find that vibrational excitation enhances $N_{2(g),v}$ dissociation on Ni but its impact on Fe is limited. Quenching of vibrationally excited $N_{2(g),y}$ due to collisions with the reactor walls and the catalyst surface does not significantly affect ammonia yields with less an order of magnitude increase. In contrast, Eley-Rideal reactions with N· and H· radicals dominate NH_{3(g)} formation, bypassing the conventional rate-controlling steps of thermal catalysis on Fe and Ni. This mechanistic picture explains the experimentally observed insensitivity ammonia production rates to catalyst identity and highlights the central role of radical chemistry in plasma-assisted ammonia synthesis.

* This work was supported by the U.S. Department of Energy, Office of Science, Office of Fusion Energy Sciences General Plasma
Science program under Award Number DE-SC-0020232.

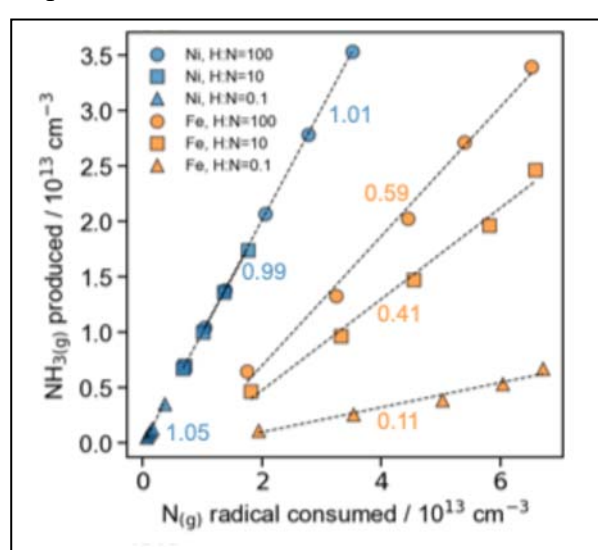


Figure 1 - Comparison between predicted NH3(g) production and N · radical consumption in a 10 mm long PBR with Fe or Ni for different H·/N· radical feed ratios. Computational details: 0.5% $N_{2(g)},\,2.5\%$ $H_{2(g)},\,97\,\%$ $Ar_{(g)}$ passes through the RF plasma reactor to generate $N_{2(g),\nu},\,H_{2(g)},\,N\cdot,$ and H· radicals as feed gas into the catalytic reactor. Total volumetric flowrate: 16.7 cm³s⁻¹; temperature: 517 K

- [1] B. Bayer; P.J. Bruggeman and A. Bhan. ACS. 13, 2619–2630 (2023).
- [2] P. Mehta; P. Barboun; F. A. Herrera; J. Kim; P. Rumbach; D. B. Go; J. C. Hicks and W. F. Schneider. Nature Publishing Group. 1, 269–275 (2018).
- [3] Y. Engelmann; K. van 't Veer; Y. Gorbanev; E. C. Neyts.; W. F. Schneider and A. Bogaerts. ACS Sustain. Chem. Eng. 9, 13151–13163 (2021).

Charging Dynamics During Pulsed Plasma Etching of High Aspect Ratio Features in Dielectric Materials *

Chenyao Huang ^a, Yeon Geun Yook ^a, Yifan Gui ^a, Steven C. Shannon ^b and Mark J. Kushner ^a

(a) University of Michigan, Ann Arbor, MI
(b) North Carolina State University, Raleigh, NC
(chenyaoh@umich.edu, scshanno@ncsu.edu, mjkush@umich.edu)

During plasma etching of high aspect ratio (HAR) features in dielectric materials (e.g., SiO₂, Si₃N₄O, ONO), disparities in the energy and angular distributions (EADs) between positive ions and electrons result in differential charging within the feature. The resulting electric fields within the feature can distort the trajectories of incoming ions resulting in defects and feature distortion. With the aspect ratio of features for memory and logic increasing, there are also increasing concerns of the consequences of charging. A proposed remedy for feature distortion due to charging is the use of pulsed biases. The feature is exposed to different fluxes and EADs of charged species during the on- and off-times during the pulse period. As a result, charging dynamics differ during the on- and off-periods. Net charging likely occurs during the on-portion of the pulsed period when ion energies are high. Discharging likely occurs during the off-portion of the period when ion energies are low, including attracting negatively charged particles into the feature.

In this work we discuss results from a computational investigation of the charging dynamics during pulsed plasma etching of HAR dielectric structures using a 3D voxel-based model, the Monte Carlo Feature Profile Model (MCFPM). MCFPM receives fluxes and EADs of incoming species toward the wafer from a model for plasma properties at the reactor scale, the Hybrid Plasma Equipment Model (HPEM). The MCFPM launches and tracks pseudoparticles representing neutral and charged fluxes towards the surface, and simulates the evolution of the feature and the charging process. The MCFPM includes newly developed algorithms for secondary electron emission processes for electrons and ions. Charging dynamics during pulsed plasma etching of HAR vias will be discussed for fluorocarbon and cyrogenic etching of SiO₂ and ONO stacks in multi-frequency capacitively coupled plasmas.

*This work was supported by the Department of Energy Office of Fusion Energy Sciences (DE-SC0024545) and Samsung Electronics.

Abstracts: Poster Session III

Heavy-Ion Plasma Properties During Rotationally-Driven Interchange Events: Insights from Juno Observations at Jupiter *

Alexandra Roosnovo and Michael Liemohn

University of Michigan (roosnovo@umich.edu)

Jupiter harbors a vast magnetic environment, known as a magnetosphere, which exemplifies a rotationally-driven plasma transport paradigm, resulting from its rapid, ~10-hour rotation and its possession of an internal heavy-ion plasma source in the moon Io. Io's volcanic output produces a dense plasma torus of sulfur-group ions which, under centrifugal stresses, unstably overlies the lower-density plasma of the outer magnetosphere. The unstable plasma configuration manifests itself dynamically through injection-like interchange events, during which the outward-moving cold and dense plasma of the inner magnetosphere is displaced by the rapid inward transport of hot and tenuous plasma from the outer magnetosphere.

Interchange events have been surveyed extensively through in-situ spacecraft measurements at Jupiter, but significant questions remain regarding the mechanisms for interchange-injection formation and the controlling factors of size and transport speed. Taking advantage of recent advancements in forward modeling of time-of-flight (TOF) data from Juno's Jovian Auroral Distributions Experiment Ion sensor (JADE-I), we conduct a statistical analysis of magnetic and heavy-ion plasma parameters during interchange-event inflows in the 10-20 R_J region (R_J = equatorial radius of Jupiter ≈ 71492 km). Events were identified as a sudden, coincident drop in total plasma density and jump in plasma temperature. Such interchange signatures tend to be clustered, with 5–15+ events occurring within a few minutes (~0.1–1 R_J) of each other, indicating either inflow splitting or that, in locally unstable regions, multiple inflows tend to generate together. We find that interchange properties display clear radial dependence, with events nearer to the planet having both higher density and lower temperature, suggesting the flows are semi-localized and originate within a few R_J of the observed signature. We evaluate ion composition and show that relative ion abundances may serve as an additional tracer of interchange inflow source location. We discuss the implications of differences in interchange properties for assessing the environmental factors which control transport in rotationally-driven planetary systems.

^{*} Work supported by the Rackham Merit Fellowship and the NASA FINESST Fellowship.

X-ray Absorption Spectroscopy Measurements of Radiatively Ionized Argon Gas*

<u>K. V. Kelso</u> ^a, S. B. Hansen ^b, H. J. LeFevre ^a, S. R. Klein ^a, P. A. Keiter ^{a,c}, R. P. Drake ^a and C. C. Kuranz ^a

- (a) University of Michigan, Ann Arbor, Michigan, 48109, USA
- (b) Sandia National Laboratories, Albuquerque, New Mexico, 87123, USA
- (c) Los Alamos National Laboratory, Los Alamos, New Mexico, 87544, USA

X-ray absorption spectroscopy is a diagnostic tool that can characterize the temperature and ionization state of a plasma. This technique requires experiments to characterize the platform, careful data calibration, and comparison with atomic models to understand the plasma parameters. We performed ionizing radiation wave experiments at the OMEGA Laser Facility that used an ~80 eV X-ray source to heat an Argon (Ar) gas cell at fill pressures of 3 atm. To diagnose the Ar plasma, we used a capsule backlighter offset 10mm from the gas cell, to produce X-rays that were absorbed by the ionized Ar gas. The absorption analysis was calibrated using the significant line structure in the backlighter spectrum, which served as independent energy fiducials enabling definitive measurements of a 50-eV shift in the energy of the Ar K-edge due to ionization. We compare the measured absorption spectra to two independent atomic models, PrismSPECT and SCRAM, and show that the observed K-edge shift in the heated gas is consistent with ionization up to Ar⁺⁴ and temperatures of 10 eV.

^{*} These experiments were conducted at the Omega Laser Facility with the beam time through the NLUF user program. This work is funded by the DOE-NNSA under cooperative agreement (No. DE-NA0004146 Sandia National Laboratories, under Contract No. DE-NA0003525.

Observations & Modeling of Subauroral Sporadic-E Plasma Irregularities

Michelle X. Bui ^a and David Hysell ^b

(a) University of Michigan (mxbui@umich.edu)(b) David Hysell (dlh37@cornell.edu)

Observations of 30-MHz coherent backscatter from subauroral sporadic-E ionization layers were obtained with a VHF imaging radar located in Ithaca, New York. The quasiperiodic (QP) echoes are similar to what has been observed at middle latitudes but with some differences. The echoes arise from bands of scatterers aligned mainly northwest to southeast and propagating to the southwest. A notable difference from observations at middle latitudes is the appearance of secondary irregularities or braids oriented obliquely to the primary bands and propagating mainly northward along them. We present a spectral simulation of the patchy layers that describes neutral atmospheric dynamics with the incompressible Navier Stokes equations and plasma dynamics with an extended MHD model. The simulation is initialized with turning shears in the form of an Ekman spiral. Ekman-type instability deforms the sporadic E layer through compressible and incompressible motion. The layer ultimately exhibits both the QP bands and the braids, consequences mainly of primary and secondary neutral dynamic instability.

^{*} Work supported by the National Science Foundation.

Femtosecond TALIF Measurements of Atomic Hydrogen in a Dielectric Barrier Discharge for Biodiesel Hydrogenation

Sankhadeep Basu^a, Anatoli Morozov^{b,c}, Arthur Dogariu^{b,d} and Hongtao Zhong^a

- (a) Department of Mechanical Engineering, Michigan State University (basusank@msu.edu) (b) Princeton Plasma Physics Laboratory
 - (c) Department of Mechanical and Aerospace Engineering, Princeton University (amorozov@princeton.edu)
 - (d) Department of Aerospace Engineering, Texas A&M University (adogariu@tamu.edu)

Atomic hydrogen plays a crucial role in low temperature plasmas, combustion and material processing as they initiate radical chemistry and facilitate energy transfer. Hydrogenation reaction, as one example, involves the addition of atomic hydrogen to unsaturated bonds (like double or triple

carbon bonds in alkenes, aromatics, and beyond) and converting them into saturated bonds (single bonds). Hydrogenation reaction is usually operated with catalyst and elevated conditions (350-450 K, 0.3 – 0.6 MPa, and 2-7 hours). Recently studies have shown that low temperature plasmas can hydrogenate biodiesel liquids with an effectiveness similar or superior to that of traditional catalytical hydrogenation[1]. Despite the progress, key intermediates, such as atomic hydrogen, has not been quantified. The reaction conditions are not readily extensible to other reactors nor are they easy to reproduce or predict.

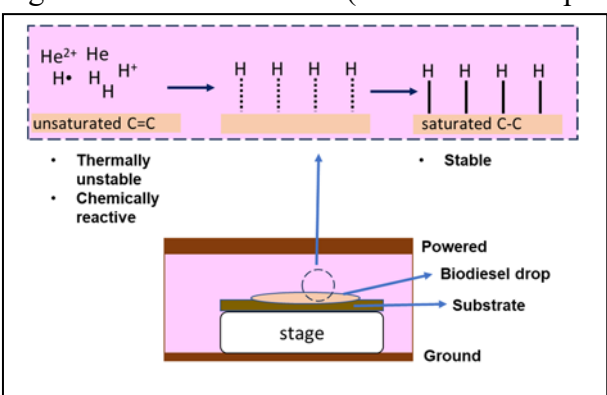


Figure 1 – Schematic of dielectric barrier discharge for biodiesel hydrogenation.

The present study measures the spatially and temporarily resolved profiles of the absolute number density of atomic hydrogen with femtosecond TALIF (two photon absorption laser induced fluorescence) and studies the plasma-initiated biodiesel hydrogenation chemistry in a dielectric barrier discharge (DBD) reactor. Based on fs-TALIF, we confirmed that the atomic hydrogen number density reaches 10¹³ cm⁻³ and the energy efficiency is high for biodiesel hydrogenation under the room temperature and 100 Torr. The plasma-initiated hydrogenation chemistry induces a spatial gradient of atomic hydrogen. Such gradients are affected by flow residence time, plasma discharge duration, and the presence of catalysts. The hydrogenation was also confirmed with gas chromatography mass spectroscopy (GC-MS) analysis of the residue biodiesel liquids, which showed a complete conversion of linoleic acid methyl ester (C18:1) to stearic acid methyl ester (C18:0). Currently a plasma chemistry modeling is ongoing to understand the underlying non-equilibrium hydrogenation mechanism.

* This work is supported by Michigan State University faculty startup and the Princeton Collaborative Low Temperature Plasma Research Facility (PCRF).

References

[1] K.-M. Lin et al., "Room-Temperature Plasma Hydrogenation of Fatty Acid Methyl Esters (FAMEs)," *Processes 2025, Vol. 13, Page 2333*, vol. 13, no. 8, p. 2333, Jul. 2025, doi: 10.3390/PR13082333.

Efficiency Mode Characterization of an Electron Cyclotron Resonance Magnetic Nozzle Thruster Operating on Nitrogen*

John Riley K. O'Toole, Ari J. Eckhaus and Benjamin A. Jorns

University of Michigan Department of Aerospace Engineering (Otoolejr@umich.edu)

There is a growing interest in operating electric propulsion (EP) systems that can operate on non-noble gas propellants, particularly as it relates to air-breathing and multimode architectures. [1] However, these missions require the use of light-weight molecular propellants that are both difficult to ionize, thus lowering performance, and pose potential lifetime risks to key aspects of mature EP devices. Most notably, for commonly flown devices like Hall-effect thrusters (HETs) and gridded ion thrusters, the electron source, the cathode, is highly susceptible to poisoning from these types of propellants.

Electron Cyclotron Resonance (ECR) thrusters, a type of wave-based plasma thruster, have the potential to overcome at least one key limitation for existing EP devices operating on unconventional fuels. This stems from the fact that ECR devices employ a largely electrodeless, non-thermionic scheme to energize their propellant. This avoids the conventional issues with poisoning attributed to Hall and gridded ion thrusters. At the same time, ECR thrusters may also offer a solution to the problem of low ionization of lightweight molecular propellants as well. Indeed, there is indirect evidence to suggest that electron temperatures in ECR devices may exceed 70 eV. [2] Such high temperatures could greatly improve ionization efficiency on molecular propellants when compared to HETs, which, at the same power levels, typically produce lower temperature electrons. [3]

To this end, we have evaluated the performance and constituent efficiency modes of a 30 W class ECR magnetic nozzle thruster operating on nitrogen. Global performance is found by thrust stand measurements, while an efficiency mode breakdown is completed with a far-field probe suite that consists of a E×B probe, a Langmuir Probe, a retarding potential analyzer, and a Faraday probe. We found that specific impulse peaked near 400 s at 50 W of input power, and total efficiency did not exceed 2%. Mass utilization, in turn, is shown to be the primary detractor to overall thruster performance. This result in the context of a mass utilization model derived by Hurley and Jorns [4] suggests that the residence time for the input nitrogen gas is around 2 μ s, suggesting that different thruster geometries and higher input powers should be explored to optimize ECR thruster performance on this propellant.

* This work was funded by the Air Force Office of Scientific Research Grant #FA9550-25-1-0025 under the Space Power and Propulsion Portfolio.

- [1] T. Andreussi et al., "A review of air-breathing electric propulsion: from mission studies to technology verification," Journal of Electric Propulsion 1, p. 31, 2022
- [2] S. Correyero et al., "Plasma Beam Characterization Along the Magnetic Nozzle of an ECR Thruster," Plasma Sources Sci. Technol. **28**, 2019
- [3] A. Smirnov, "Plasma Measurements in a 100 w Cylindrical Hall Thruster," Journal of Applied Physics, 2003.
- [4]W. J. Hurley and B. A. Jorns, "Mass utilization scaling with propellant type on a magnetically shielded hall thruster," Plasma Sources Sci. Technol. **34**, 055010, 2025.

Boundary Layer Phenomena in Mercury's Magnetosphere

Sarah Feldman and Jim Raines

University of Michigan, Climate & Space Sciences Department (sarfeldm@umich.edu, jraines@umich.edu)

The MErcury Surface, Space ENvironment, GEochemistry, and Ranging (MESSENGER) mission's Fast Imaging Plasma Spectrometer (FIPS) orbited Mercury from 2011 to 2015, measuring planetary ions and sampling its magnetospheric plasma. Mercury's magnetic field is significantly more dynamic than Earth's, resulting in magnetic reconnection rates that are an order of magnitude faster and a two-minute Dungey cycle. This configuration is the result of the planet's proximity to the Sun combined with its weak magnetic field.[1] Mercury's highly variable magnetosphere gives rise to boundary layer structures, which are found between two regions of differing plasma properties, and can provide insight about how ions flow around the planet.

This work utilizes FIPS data from MESSENGER orbits to look at several different boundary layers with the goal of identifying different processes that could be occurring in them, as well as finding more. Disappearing Dayside Magnetopause (DDM) events were investigated, with four being previously identified.[2] Due to asymmetries in Mercury's magnetic field, MESSENGER orbits were filtered based on proximity to the dayside southern hemisphere, a region where the magnetopause could completely disappear. We also investigate Mercury's nightside and attempt to identify Mercury's Nightside Plasma Sheet Boundary Layer (NPSBL) and differentiate it from the plasma sheet and its horns. Preliminary results show a persistent feature on the nightside, near the equator and within 1 R_M in the X-direction using MSO coordinates. This feature is characterized by rapid magnetic field oscillations and a dropout of lower-energy particles. Before its identification as the PSBL, further analysis is needed. Ongoing research may expand to investigate other boundary layers of interest, such as Low Latitude Plasma Boundary Layers.

References

[1] Raines, J. M., et al. (2012), Distribution and compositional variations of plasma ions in Mercury's space environment: The first three Mercury years of MESSENGER observations, J. Geophys. Res. Space Physics **118**, 1604–1619, doi:10.1029/2012JA018073.

[2] Slavin, J. A., Middleton, H. R., Raines, J. M., Jia, X., Zhong, J., Sun, W.-J., et al (2019). MESSENGER observations of disappearing dayside magnetosphere events at Mercury. Journal of Geophysical Research: Space Physics **124**, 6613–6635. https://doi.org/10.1029/2019JA026892

PFAS Degradation in Water using Atmosphere Pressure Plasmas*

<u>Jisu Jeon</u> ^a, Tiago C. Dias ^a, Xuefei Qiu ^b, Stephen Olson ^c, Selma Mededovic-Thagard ^b and Mark J. Kushner ^a

(a) University of Michigan, Ann Arbor, MI 48109 USA(b) Clarkson University, Potsdam, NY 13699 USA(c) 3M Company, Saint Paul, MN 55144 USA

Long-chain per- and polyfluoroalkyl substances (PFAS) are forever chemicals persistently residing at the water surface and can be defluorinated by chemically activating the liquid using Atmospheric pressure plasmas (APPs) [1]. APPs launches surface ionization waves (SIWs) near

the liquid surface, where energetic electrons, ions and VUV photons can directly impact and generate solvated electrons in water. PFAS molecules having a low acid-dissociation constant K_a mainly exist in their conjugate bases and are degraded through decarboxylationhydroxylation-elimination-hydrolysis (DHEH) mechanism, which is driven by electrons, ions, photons, and solvated electrons. In this work, the degradation of surfactant molecules PFAS by APPs was investigated using 2-D (nonPDPSIM) and 0-D (GlobalKin). The SIWs on the water surface was studied in the 2-D model and the gas fluxes arriving to the surface were implemented to the 0-D model to investigate the degradation of PFOA over minutes timescales. defluorination rates were evaluated based on voltages, repetition rates, and flow rates.

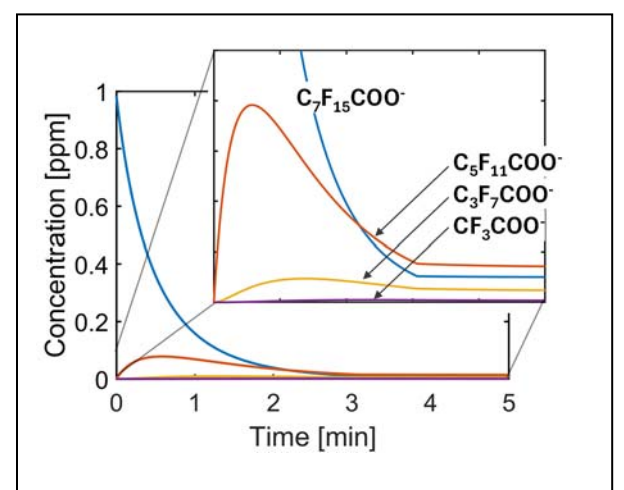


Figure 1 – PFOA and and degradated products by DHEH (decarboxylation-hydroxylationelimination-hydrolysis) mechanism

* This work was supported by the US Department of Energy Office of Fusion Energy Sciences (DE-SC0020232), the Army Research Office MURI program (W911NF-20-1-0105), the National Science (CBET 2032604) and the 3M Company.

References

[1] Mikhail Vasilev et al, Chemical Engineering Journal 473 (2023) 144833.

Mean Force Kinetic Theory of Warm Dense Matter*

Lucas Babati ^a, Nathaniel Shaffer ^b and Scott Baalrud ^a

- (a) University of Michigan, Ann Arbor, MI
- (b) Laboratory for Laser Energetics, Rochester, NY

To run large scale hydrodynamic simulations of plasmas for inertial confinement fusion or planetary sciences, transport coefficients must be known analytically or be easily looked up in a table. This is known for gas-like or solid-like plasmas, but in the warm dense matter range, the transport properties are either not well known or expensive to calculate. We present a method based on Mean Force Kinetic Theory [1] to calculate transport coefficients which extends typical plasma theory into the strongly coupled regime. We use the Strongly Coupled Transport Code (SCOUT) to solve a Chapman-Enskog expansion of a classical kinetic equation to describe ionic transport with the effect of degenerate electron screening provided by the Average Atom Two Component Plasma (AA-TCP) model [2]. For electronic transport, an analogous semi-classical kinetic equation is used along with fully quantum mechanical scattering. Calculations of viscosity, conductivity, and stopping power are presented using SCOUT and compared against other theories.

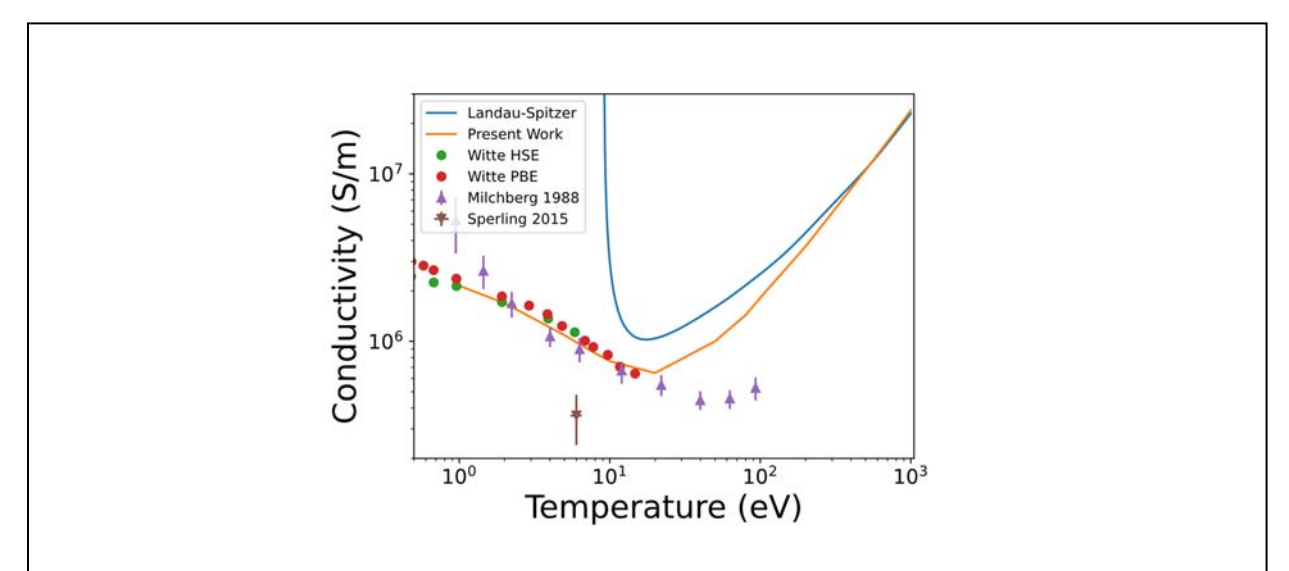


Figure 1 - Witte points are QMD results using Heyd-Scuseria-Ernzefhof (HSE) and Perdew-Burke-Ernzerhof (PBE) exchange correlation functionals [3], Landau-Spitzer is the classical result [4], Milchberg [5] and Sperling [6] are experimental measurements.

- [1] S. D. Baalrud and J. Daligault, Phys. Plasmas 26, 082106 (2019).
- [2] C. E. Starrett and D. Saumon, HEDP 10, 35-42 (2014).
- [3] B. B. L. Witte et al. Phys. Plasmas. 25, 056901 (2018).
- [4] Spitzer, Physics of Fully Ionized Gases (1956).
- [5] H. Milchberg et al. Phys. Rev. Lett. **61**, 2364 (1998).
- [6] P. Sperling et al. Phys. Rev. Lett. 115, 115001 (2015).

^{*} This work is funded by the U.S. Department of Energy NNSA Center of Excellence under cooperative agreement number DE-NA0004146 and by the Department of Energy [National Nuclear Security Administration] University of Rochester "National Inertial Confinement Fusion Program" under award No. DE-NA0004144.

Experimental Characterization of the Co-Axial Electrodeless Magnetoplasmadynamic Thruster*

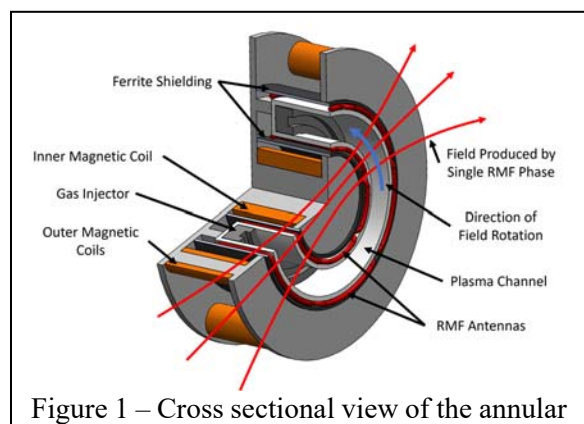
Grace Zoppi, Dr. Tate Gill, Dr. Christopher Sercel and Benjamin Jorns

Department of Aerospace Engineering at the University of Michigan (gzoppi@umich.edu)

One of the key metrics for advanced electric propulsion concepts is high power densities enabling large power levels without employing prohibitively massive thruster technologies. The Applied Field MPD (AF-MPD) thruster, a type of Lorentz force accelerator, has long been considered a leading choice for this purpose. However, one of the largest impediments to AF-MPD thrusters has been thruster lifetime. The DC electrodes on these devices are subject to an extreme plasma environment and thus erode rapidly. To mitigate this issue, the Plasmadynamics and Electric Propulsion Laboratory has previously conducted research into utilizing a Rotating Magnetic Field (RMF) to inductively drive the azimuthal current, a major component of the Lorentz force generation in a nominal AF-MPD thruster. This has created a new thruster

architecture which we have coined the electrodeless magnetoplasmadynamic (E-MPD) thruster.

In a previous test campaign, demonstrated the performance of a three-phase RMF-driven thruster in a continuous-wave operation and measured a peak efficiency of 2.6% and specific impulse of 575s on xenon [1]. Given this limited performance, a steady state CFD model was developed to illuminate design strategies to improve thruster performance. These design strategies motivated an annular E-MPD design, a pivot from the previously tested conical



E-MPD thruster.

geometries [2]. Fig 1 shows the new annular test article, which is experimentally characterized in this work to validate predicted performance improvements. This is achieved by collecting data from a retarding probe analyzer and current transducers in a low vacuum environment, intended for rapid test iterations. These diagnostics respectively provide the ion velocity distribution function and RMF antenna waveforms. The resulting analysis enables a direct comparison with probe measurements from the conical prototype E-MPD and offers new insights into scaling laws for RMF-driven thrusters, guiding future design improvements.

*Work supported by NASA Grant 80NSSC24K1334.

- [1] C Sercel, "Characterization of Performance and Current Drive Mechanism for the Rotating Magnetic Field Thruster," PhD thesis. University of Michigan. (2023).
- [2] G Zoppi, T Gill, C Sercel, and B Jorns, "The Design and Characterization of a Co-Axial Electrodeless Magnetoplasmadynamic Thruster," AIAA SCITECH 2025 Forum. (2024). https://doi.org/10.2514/6.2025-2039.

Effects of Resistivity and Radiative Losses on Magnetic Reconnection in MHD* Ian Freeman and Brian O'Shea

Michigan State University (freem386@msu.edu)

Many magnetic reconnection studies investigate magnetic reconnection in MHD using constant or spatially varying anomalous diffusivity terms. Some have investigate the effects of temperature-varying diffusivity, and found enhanced reconnection rates. Similar studies and results have been found when radiative effects are considered. Using the non-ideal MHD code AthenaPK we investigate the effects and differences on the inclusion of different diffusion models and radiative effects on magnetic reconnection in laboratory-like environments. Performing a large parameter sweep of Spitzer conductivities and radiative loss coefficients we find enhanced reconnection rates when Spitzer conductivity and radiation are enabled when compared to the standard ohmic diffusion models.

* This work is supported in part by the National Science Foundation Research Traineeship Program (DGE-2152014) to Ian Freeman.

- [1] R. Datta, K. Chandler, et. al., Phys. Plasmas 31 (5): 052110 (2024).
- [2] Petschek, H. E. 1964, NASA Special Publication 50, 425 (1964).

Spectral Line Widths in Plasmas using an Average Atom Model*

Julian Kinney ^a, Stephanie Hansen ^b, Thomas Gomez ^a and Scott Baalrud ^a

(a) University of Michigan (julkin@umich.edu) (b) Sandia National Laboratories

Accurate spectral line broadening calculations are important for both simulation and experimental diagnosis of plasmas in nuclear fusion, astrophysical objects, and semiconductor manufacturing. This work uses the impact approximation framework to calculate how the spectral line of the 2p1s²-2s1s² transition in Boron-III is broadened by electrons in a plasma. In the impact approximation, the spectral line width is computed by averaging electron impact excitation and deexcitation cross sections over an electron distribution function.[1] First, it is shown that when the free electron wavefunctions are calculated using a self-consistent Average-Atom potential, the cross

sections include resonances due to pressureionized bound states. Second, modification of the free electron wavefunctions produces significantly different line widths as density increases (see Fig. 1). Finally, the calculation method here is compared with reduced models that are traditionally used in line broadening calculations.

* This work is funded by the DOE NNSA Stockpile Stewardship Graduate Fellowship through cooperative agreement DE-NA0003960.

References

[1] M. Baranger, "General impact theory of pressure broadening," Phys. Rev. **112**, 855–865 (1958).

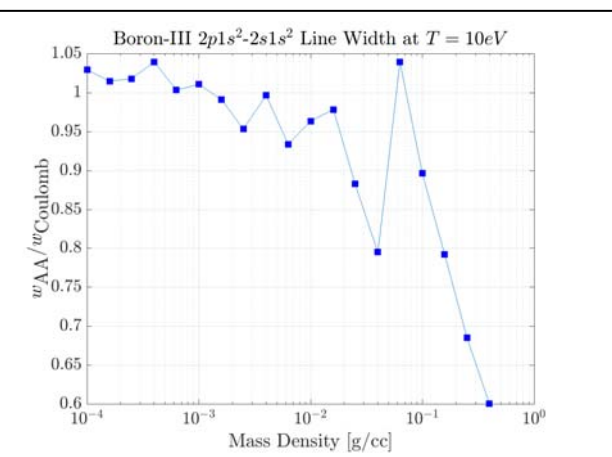


Figure 1 – Ratio of two spectral line widths calculated using the free electorn wavefunctions from the self-consistent Average-Atom and Coulomb potentials. The two methods produce significantly different results as density increases.

Controlling Energetic Neutral Beams Produced from Inductively Coupled Plasmas for Material Processing Applications*

Gonçalo Cardoso and Mark Kushner

University of Michigan, 1301 Beal Avenue, Ann Arbor, MI 48109-2122, USA

Plasma etching and deposition are essential for microelectronics fabrication. Precise control of energy and angular distributions (EADs) of ions accelerated onto biased wafers is required to stimulate critical surface chemical reactions. However, charge buildup in the etched feature can perturb ion trajectories or damage the electronic device. This is particularly the case for fabrication of 2-dimensional devices that consist of nearly monolayer thickness. Energetic neutral beams have been proposed as a damage-free technique for etching and deposition [1]. These are often produced by first accelerating ions, followed by reflection and neutralization on the walls of apertures of a biased grid.

In this paper we discuss results from a computational investigation of the properties of neutral beams produced in inductively coupled plasmas. The Plasma Chemistry Monte Carlo Module (PCMCM) in the Hybrid Plasma Equipment Model (HPEM) has been improved to track the motion of ions as they neutralize on and reflect from a grid, and collide with background particles before reaching the wafer. Typical conditions are pressures of tens of mTorr, gas mixtures containing Ar, Cl2 or O2 and biases of hundreds of volts. The effect of aperture aspect ratio, bias, pressure and gas mixture on the neutralization efficiency and neutral EADs will be discussed.

* Work supported by the U.S. Department of Energy, Office of Science, Fusion Energy Sciences (FES) and Basic Energy Sciences (BES).

References

[1] S. Samukawa, ECS J. Solid State Sci. Technol. 4 (6), N5089-N5094 (2015).

Space-Charge and Circuit-Induced Distortion of Short-Pulse Beams in a Vacuum Diode

Yves Heri and Peng Zhang

University of Michigan, Ann Arbor, MI, USA (heriyves@umich.edu)

The dynamics of short-pulse electron beams in vacuum diodes are strongly influenced by both space-charge effects and the interaction with the external driving circuit. Unlike free-drift propagation, in a diode configuration the coupling between the emission current and the voltage drop across the gap leads to additional nonlinear temporal distortions of the pulse. As the instantaneous current increases, the charge accumulation within the gap modifies the electric field at the cathode, inducing feedback that affects both the emission and transport processes. When the

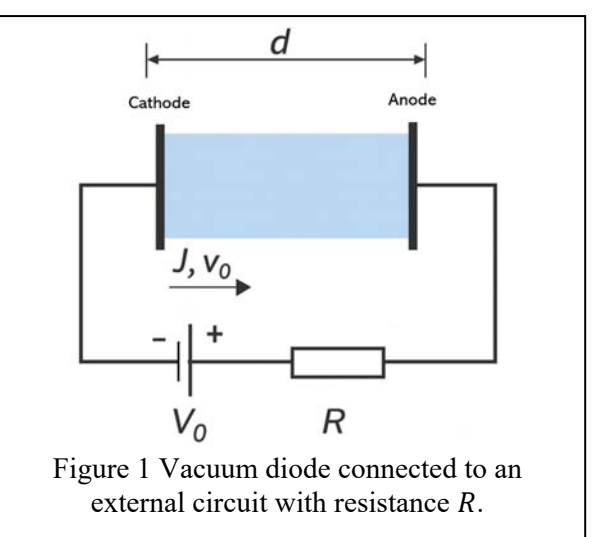
diode is connected to a circuit with finite impedance, such as a series resistance R or load impedance Z, the voltage waveform across the gap evolves dynamically according to

$$V_q(t) = V_0 - RI(t) \tag{1}$$

where I(t) is the sum of the conduction and displacement current. For M discrete charge sheets, where ρ_i and v_i represent the charge density and velocity of the i-th sheet, respectively, the total current can be expressed as

$$I(t) = \frac{A}{d} \sum_{i}^{M} \rho_{i} v_{i} + \frac{\varepsilon_{0} A}{d} R \frac{dI(t)}{dt}$$
 (2)

In this work, a gridless multiple-sheets



solver is developed to self-consistently calculate the electric field, charge transport, and circuit evolution in a vacuum diode. The framework enables systematic investigation of how external impedance, emission profiles, pulse duration, diode gap distance, applied voltage, and initial emission velocity jointly influence beam broadening, waveform distortion, and current dynamics. The work focuses on deriving scaling laws and benchmarking the model against particle-based

intended to extend this work in a plasma gap in the near future.

simulations to quantify circuit-modified space-charge effects in short-pulse beam diodes. It is

* Work is supported by the Air Force Office of Scientific Research (AFOSR) Grant No. FA9550-20-1-0409, the Air Force Office of Scientific Research (AFOSR) Award No. FA9550-22-1-0523, and Grant No. 2516752.

- [1] Y. Heri and P. Zhang, IEEE Trans. Electron Devices **72**(5), 2591–2596 (2025).
- [2] P. Zhang et al., Appl. Phys. Rev. 4(1), 011304 (2017).

Control of Magnetic Reconnection in Laser Plasma Interaction*

Joshua L. Latham ^a, Brandon K. Russell, ^b Chuanfei Dong, ^c Christopher A. Walsh, ^d Kyle G. Miller, ^e Paul T. Campbell, ^a Louise Willingale, ^a Philip Nilson, ^e and Karl M. Krushelnick ^a

- (a) Center for Ultrafast Optical Science, University of Michigan, Ann Arbor, MI 48109, USA (joshla@umich.edu)
- (b) Department of Astrophysical Sciences, Princeton University, Princeton, NJ 08544, USA (c) Center for Space Physics and Department of Astronomy, Boston University, Boston MA 02215, USA
 - (d) Lawrence Livermore National Laboratory, 7000 East Avenue, Livermore, CA 94550, USA
 - (e) Laboratory for Laser Energetics, University of Rochester, Rochester, NY 14623, USA

We conducted an experiment in order to control laser-driven magnetic reconnection (MR) using an external perturbation provided by a short pulse (SP) laser. The SP impinged on the current sheet between two colliding laser-driven, self-magnetizing plasma plumes.

We found that the short pulse laser in one case injected a large plasma-magnetic structure into the current sheet, while in another case it caused a forward-jump in the usual MR timeline, annihilating magnetic flux and causing instabilities in the current sheet between the two plasma plumes.

We conclude that it may be possible to tune the external control of laser-driven MR, depending on the proper (1) SP laser energy and (2) plasma density profile at the time of

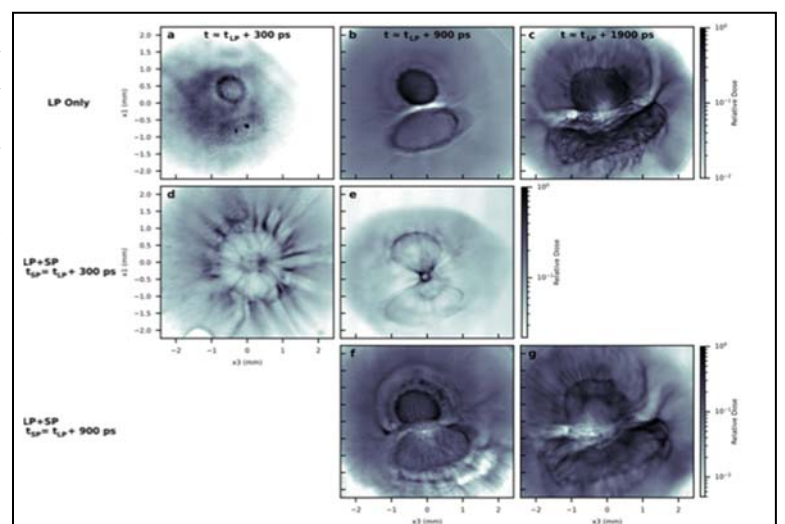


Figure 1 – Experimental proton radiographs, scaled to object plane. Panes **a-c** show the development of the ultraviolet long pulse (LP) driven plumes without any short pulse (SP). Panes **-e** show the case of firing the SP at $t = t_{LP} + 300$ ps, and **f-g** show the case of firing the SP at $t = t_{LP} + 900$ ps. Each column of radiographs represents approximately the same amount of total LP drive.

the SP laser's arrival. Additionally, hot electrons generated by the SP can have magnetic effects that extend beyond the SP focal spot, providing an additional mechanism to influence MR in the laboratory.

These results are relevant to understanding the onset and dynamic evolution of reconnection current sheets under external perturbations, with broader implications for space and astrophysical plasmas.

* The experiment was conducted at the Omega Laser Facility with beam time through the National Laser Users' Facility (NLUF) (or the Laboratory Basic Sciences) under the auspices of the U.S. DOE/NNSA by the University of Rochester's Laboratory for Laser Energetics under Contract DE-NA0003856.

Vlasov-Poisson Simulations of Ion Acoustic Waves

Jiashu Han, Robert Krasny and Alexander Thomas

University of Michigan (shujhan@umich.edu)

We present simulations of ion acoustic waves in a 1D1V spatially periodic domain using an extended version of the FARSIGHT Vlasov-Poisson code, adapted for two-species plasmas. FARSIGHT is a forward semi-Lagrangian scheme with 4th order Runge-Kutta time-stepping and a tree-based adaptively refined particle/panel representation of the distribution functions in phase space. Unlike the particle-in-cell (PIC) method, FARSIGHT computes the electric field as a regularized convolution integral in phase space using a GPU-accelerated barycentric Lagrange treecode. Our results include studies with varying electron-to-ion temperature ratios (Te/Ti), and we report on several key diagnostics: the damping rate of the electric field, plasma frequency, electron and ion charge densities, and the phase space distribution functions of both species. A recurring irregular feature was observed in the time evolution of the 2-norm of the electric field, exhibiting a temporal period that appears to depend on the maximum velocity of the simulation domain. The cause of this feature is currently under investigation.

Curvature-Enhanced Quantum Tunneling Emission in Dissimilar Metal-Insulator-Metal Junctions*

Bingqing Wang and Peng Zhang

Department of Nuclear Engineering and Radiological Sciences, University of Michigan, Ann Arbor, Michigan 48109-2104, United States

We developed a self-consistent quantum tunneling electron emission framework [1] for dissimilar metal-insulator-metal (MIM) nanogaps [2] and use it to compare the tunneling process for planar and cylindrical (coaxial) geometries under different applied bias voltage. The model couples a Schrödinger-Poisson solver to a WKBJ electron transmission through a barrier that includes work-function mismatch, cylindrical/planar image charge potential lowering, exchange correlation, and space-charge feedback. Emission from both electrodes is computed with freeelectron model based supply functions, yielding polarity-dependent forward/reverse currents and a unified map of direct tunneling, field emission, and quantum space-charge-limited regimes. Relative to the planar case, curvature in the cylindrical gap introduces geometric field focusing (\alpha 1/r) and a logarithmic background potential, which together narrow and lower the effective barrier, enhance cathode-dominated emission, and shift boundaries between different emission regimes to lower voltages. Systematic sweeps over gap size, radius ratio $\eta = r_2/r_1$, dielectric constant, and work-function contrast reveal simple scaling laws for onset current (in context of field emission) and asymmetry. The results provide insights into the dependence of tunneling and emission on gap geometry and demonstrate how curvature can be exploited to boost tunneling and field-emission performance in nanowire contacts[3], coaxial nanojunctions, and curved-tip emitters[4].

* The work is supported by the Air Force Office of Scientific Research (AFOSR) Award No. FA9550-22-1-0523.

- [1] P. Zhang, Scientific reports 5, 9826 (2015).
- [2] Banerjee, S. and Zhang, P., 2019. AIP Advances 9, no. 8, 085302 (2019).
- [3] B. Wang, S. Banerjee, and P. Zhang, ACS Appl. Electron. Mater., 7, 1192–1201 (2025).
- [4] S. B. Fairchild et al., IEEE Transactions on Plasma Science, vol. 47, no. 5, pp. 2032-2038 (2019)

List of Participants

First name	Last name	Email	University
Ibukunoluwa	Akintola	iakintol@nd.edu	ND
Madison	Allen	mgallen@umich.edu	U-M
Lucas	Babati	lbabati@umich.edu	U-M
Sankhadeep	Basu	basusank@msu.edu	MSU
Declan	Brick	brickd@umich.edu	U-M
Khalil	Bryant	kalelb@umich.edu	U-M
Michelle	Bui	mxbui@umich.edu	U-M
Alexander	Cushen	atcushen@umich.edu	U-M
Briggs	Damman	bdamman@umich.edu	U-M
Bineet	Dash	bkdash@umich.edu	U-M
Ari	Eckhaus	aeckhaus@umich.edu	U-M
Md Arifuzzaman	Faisal	faisalmd@umich.edu	U-M
Sarah	Feldman	sarfeldm@umich.edu	U-M
lan	Freeman	freem386@msu.edu	MSU
Yifan	Gui	evangyf@umich.edu	U-M
Jiashu	Han	shujhan@umich.edu	U-M
Yves	Heri	heriyves@umich.edu	U-M
Chenyao	Huang	chenyaoh@umich.edu	U-M
Mitchell	Indek	mindek@umich.edu	U-M
Jisu	Jeon	jisujeon@umich.edu	U-M
Lan	Jin	jinlan@umich.edu	U-M
Nicolas	Kalem	nmontyk@umich.edu	U-M
Kwyntero	Kelso	kkelso@umich.edu	U-M
Kyle	Kemmerer	kylekem@umich.edu	U-M
Julian	Kinney	julkin@umich.edu	U-M
Joshua	Latham	joshla@umich.edu	U-M
Amelia	Lee	ameliale@umich.edu	U-M
Jarett	LeVan	jarettl@umich.edu	U-M
Wencheng	Lin	linwenc1@msu.edu	MSU
Evan	Litch	elitch@umich.edu	U-M
Miron	Liu	mironliu@umich.edu	U-M
Alexander	Loomis	loomisa6@msu.edu	MSU
Md	Mashrafi	mdmash@umich.edu	U-M
William	Maxon	wmaxon@umich.edu	U-M
Gonçalo Amadeu	Mendes Cardoso	gcardoso@umich.edu	U-M
Horacio	Moreno Montanes	hmorenom@umich.edu	U-M
Oluwatosin	Ohiro	oohiro@umich.edu	U-M
John Riley	O'Toole	otoolejr@umich.edu	U-M
Ryan	Park	rmpark@umich.edu	U-M
Md Wahidur	Rahman	rahman63@msu.edu	MSU
Alexandra	Roosnovo	roosnovo@umich.edu	U-M

First name	Last name	Email	University
Andrew	Schok	aaschok@umich.edu	U-M
Mary	Smirnova	marysgk@umich.edu	U-M
Cole	Stewart	stewa873@msu.edu	MSU
Chelsea	Tischler	chemay@umich.edu	U-M
Nolan	Tribu	ntribu@umich.edu	U-M
Bingqing	Wang	bqwang@umich.edu	U-M
James	Welch	welchjc@umich.edu	U-M
Yeon Geun	Yook	ygyook@umich.edu	U-M
Grace	Zoppi	gzoppi@umich.edu	U-M